Euro. Jnl of Applied Mathematics (2006), *vol.* 17, *pp.* 525–556.
doi:10.1017/S095679250600667X First published online 21 December 2006 Printed in the United Kingdom

Explicit stationary solutions in multiple well dynamics and non-uniqueness of interfacial energy densities

NICHOLAS D. ALIKAKOS[1], SANTIAGO I. BETELÚ[2] and XINFU CHEN[3]

[1]*Mathematics Department, University of Athens, Panepistimiopolis, Athens 11584 Greece*
email: nalikako@earthlink.net
[2]*Department of Mathematics, University of North Texas, Denton, TX 76203, USA*
email: betelu@unt.edu
[3]*Department of Mathematics, University of Pittsburgh, Pittsburgh, PA 15260, USA*
email: xinfu+@pitt.edu

(*Received 25 October 2005; revised 24 July 2006*)

We present a theory that enables us to construct heteroclinic connections in closed form for $2\mathbf{u}_{xx} = W_{\mathbf{u}}(\mathbf{u})$, where $x \in \mathbb{R}$, $\mathbf{u}(x) \in \mathbb{R}^2$ and W is a smooth potential with multiple global minima. In particular, multiple connections between global minima are constructed for a class of potentials. With these potentials, numerical simulations for the vector Allen-Cahn equation $\mathbf{u}_t = 2\epsilon^2\Delta\mathbf{u} - W_{\mathbf{u}}(\mathbf{u})$ in two space dimensions with small $\epsilon > 0$, show that between any fixed pair of phase regions, interfaces are partitioned into segments of different energy densities, where the proportions of the length of these segments are changing with time. Our results imply that for the case of triple-well potentials the usual Plateau angle conditions at the triple junction are generally violated.

1 Introduction

In this paper we study solutions to

$$2\mathbf{u}_{xx} - W_{\mathbf{u}}(\mathbf{u}) = 0 \ \text{ in } \ \mathbb{R}, \qquad \lim_{|x|\to\infty} W(\mathbf{u}(x)) = 0 \tag{1.1}$$

where $\mathbf{u} = (u^1, \ldots, u^N)$ is a vector valued function from $\mathbb{R}$ to $\mathbb{R}^N$ and $W_{\mathbf{u}} = (\frac{\partial W}{\partial u^1}, \ldots, \frac{\partial W}{\partial u^N})$ where $W : \mathbb{R}^N \to \mathbb{R}$ is a (smooth) function satisfying

$$W > 0 \ \text{ in } \mathbb{R}^N \setminus A, \quad W = 0 \ \text{ on } A = \{\mathbf{a}_1, \ldots, \mathbf{a}_n\}, \quad \liminf_{|\mathbf{u}|\to\infty} W(\mathbf{u}) > 0.$$

The equations in (1.1) can be regarded as Newton's equations of motion for N material points of equal mass under the potential $-W(\mathbf{u})$, with x standing for time and $|\mathbf{u}_x|^2$, $-W(\mathbf{u})$ the kinetic and potential energy, respectively. Alternatively, the Hamiltonian formulation captures the motion from one well of the potential to another is a critical point of the

action functional

$$E(\mathbf{u}) := \tfrac{1}{2}\int_{\mathbb{R}} \Big(|\mathbf{u}_x|^2 + W(\mathbf{u}) \Big) dx \tag{1.2}$$

with (1.1) being the associated Euler-Lagrange equation.

In what follows A is called the **set of wells** and for a solution $\mathbf{u}$ to (1.1) with

$$\mathbf{a}_i = \lim_{x\to-\infty} \mathbf{u}(x), \qquad \mathbf{a}_j = \lim_{x\to\infty} \mathbf{u}(x),$$

the set $\{\mathbf{u}(x) \mid x \in \mathbb{R}\}$ is referred to as a **connection** or **trajectory** connecting $\mathbf{a}_i$ and $\mathbf{a}_j$.

For $N = 1$, constructing connections is elementary and is done either by utilizing the first integral of (1.1) or by phase plane analysis [27, 30, 7]. For general $N > 1$ the connection problem is difficult and has been analyzed only for certain special potentials. In the present paper we restrict ourselves to $N = 2$. Thus, we study the O.D.E. system

$$2u^1_{xx} = \frac{\partial W(u^1, u^2)}{\partial u^1}, \qquad 2u^2_{xx} = \frac{\partial W(u^1, u^2)}{\partial u^2}.$$

Utilizing Jacobi's geometric version of the least action principle (cf. [25, 34]) that relates the critical points of E to the critical points of the parametric functional (transition energy)

$$E_1(\mathbf{u}) = \int |\mathbf{u}_x| \sqrt{W(\mathbf{u})}\, dx$$

and employing complex analysis methods we can solve the connection problem (1.1) and furthermore produce explicit solutions for a variety of potentials. In our approach we employ $\mathbb{C}$ as a phase space and use a first integral of (1.1) corresponding to the principle of equipartition of mechanical energy.

We can handle two kinds of potentials. Write

$$z = u^1 + \mathbf{i}u^2, \quad \mathbf{i} = \sqrt{-1}, \quad W(u^1, u^2) = |f(z)|^2,$$

A potential is of **type I** if f is holomorphic and of **type II** if $f(z)$ is meromorphic single-valued or multiple valued with poles. (We remark that potentials of this form include the natural class of potentials given as products of squares of distances from a finite set of points, $\Pi_{i=1}^n |z - z_i|^2$.)

For type I potentials, we show that there exists at most one connection between any pair of wells. For type II potentials, multiple connections between a pair of wells may exist. Here the poles play the role of obstacles and depending on the side we shoot from, we obtain the one or the other connection. Indeed the first evidence of the existence of multiple connections was numerical and based on a shooting method. Finally the potential with the poles can be smoothened out near the poles without affecting the connections (since they do not go through the pole) hence rendering a C^∞ potential.

Particularizing to the following two potentials

$$W_I(\mathbf{u}) = |z^3 - 1|^2, \qquad W_{II}(\mathbf{u}) = \frac{|z^3 - 1|^2}{|z^3 + \alpha^3|},$$

https://doi.org/10.1017/S095679250600667X Published online by Cambridge University Press

where α is a positive parameter, we can state the following:

- for W_I we construct a unique connection in closed form between any pair of points from the set $A = \{1, e^{2\pi i/3}, e^{-2\pi i/3}\}$ of wells;
- for W_{II} we show that there exist two connections for each pair of points from A. Both connections correspond to local minima of E and are constructed in closed forms. Depending on α, either connection can be energetically more efficient.

We also provide several other examples of potentials including

- a potential with no connection between two of its wells and
- a potential with a connection that makes a specified number of loops around a pole.

Our study of (1.1) is motivated by the vector Allen-Cahn equation

$$\mathbf{u}_t = 2\epsilon^2 \Delta \mathbf{u} - W_{\mathbf{u}}(\mathbf{u}), \qquad \mathbf{u} : \Omega \times (0, \infty) \to \mathbb{R}^2 \tag{1.3}$$

where Ω is a domain in $\mathbb{R}^2$ and W is a multiple-well potential. This system is known to be capable of simulating the evolution of grain boundaries. It is a gradient flow of the energy functional

$$\int_\Omega \left\{ \epsilon^2 |\nabla \mathbf{u}|^2 + W(\mathbf{u}) \right\} dx.$$

For small $\epsilon > 0$, one expects that typical initial data will evolve quickly at an $O(1)$ time scale towards the set A of wells, so that the domain Ω soon is partitioned into **phase regions** in each one of which $\mathbf{u}$ is approximately constant. These regions are separated by thin zones, the **diffuse interfaces**, of width $O(\epsilon)$. Subsequently, these interfaces start evolving by mean curvature at an $O(\epsilon^{-2})$ time scale. At a *junction*, the meeting point of three interfaces, the angles attain certain values that remain fixed as long as the junction exists. We refer to [14, 16] for formal, numerical and rigorous evidence supporting these scenarios, and to [31] for the study of the geometric problem.

The structure of $\mathbf{u}$ near the interface and away from the junction is essentially 1-dimensional, varying only in the direction perpendicular to the interface with a profile close to a scaled version of a solution of (1.1) [14]. This is plausible since at the interface the Laplacian and the free term balance each other, to principal order in ϵ, and thus (1.1) is satisfied approximately. The angle conditions are determined by the transition energies connecting the pairs of the states [14].

We point out some of the implications of the non-uniqueness and the non-existence of connections. On the positive side the examples of symmetric potentials that exhibit non-uniqueness establish the conjecture made in Alama *et al.* [3] that this phenomenon can occur, and substantiate the main result in that paper which presupposes non-uniqueness. On the negative side, the non-existence examples show that the statement in lemma 1 in Bronsard & Reitich [14] that any pair of global minima in a triple-well potential can be connected as a byproduct of the work in [34] is false. Also, the non-uniqueness example for a symmetric potential (example 7) that possesses two connections for each pair of minima with unequal energies shows the assertion in Sternberg [14] p. 357 which is a common perception that the Plateau angles should always be 120° is false. Indeed the

https://doi.org/10.1017/S095679250600667X Published online by Cambridge University Press

angles are determined by the formula 5 of Bronsard & Reitich [14],

$$\frac{\sin\theta_1}{\Phi^{ca}} = \frac{\sin\theta_2}{\Phi^{ab}} = \frac{\sin\theta_3}{\Phi^{bc}}$$

which shows clearly that if $\Phi^{ab} \neq \Phi^{ac}$ the angles can not all be equal. We note that the non-uniqueness and non-existence are robust under perturbations of the potential (examples 3 and 9).

In Figure 1 we present a simulation for (1.3) with $W(\mathbf{u}) = |z^3 - 1|^2/|z^3 + \alpha^3|$. It shows clearly the existence of interfaces possessing " black" and "white" partitions corresponding to one or the other connection. By adjusting the parameter α we can achieve coexistence of these profiles for a long time, or we can make the one or the other disappear very quickly.

All these facts are in sharp contrast to the well-known scalar version of (1.3), where the associated geometric evolution is motion by curvature and is insensitive to the specifics of the potentials. We shall pursue these issues on (1.3) in a subsequent paper [5].

Our method of construction of the connections can be adapted to

$$q\left(|\mathbf{u}_x|^{p-2}\mathbf{u}_x\right)_x - W_{\mathbf{u}}(\mathbf{u}) = 0, \qquad p > 1, \quad \frac{1}{p} + \frac{1}{q} = 1, \tag{1.4}$$

that, up to a scaling, is the one-dimensional steady state of the vector equation

$$\mathbf{u}_t = q\epsilon^2 \operatorname{div}\left(|\nabla\mathbf{u}|^{p-2}\nabla\mathbf{u}\right) - W_{\mathbf{u}}(\mathbf{u}). \tag{1.5}$$

We close this introduction by sketching our method for the standard triple-well potential $W(z) = |z^3 - 1|^2$. Here, $A = \{1, e^{2\pi\mathbf{i}/3}, e^{-2\pi\mathbf{i}/3}\}$. For definiteness we construct the connection between $\mathbf{a} = 1$ and $\mathbf{b} = e^{2\pi\mathbf{i}/3}$, by considering the variational problem for $E_1(\mathbf{u}) = \int |\mathbf{u}_x|\sqrt{W(\mathbf{u})}dx$ along embeddings in the plane connecting $\mathbf{a}$ to $\mathbf{b}$. Since the specific parametrization is not important we chose $\mathbf{u} : (0,1) \to \mathbb{R}^2$ with $\mathbf{u}(0) = \mathbf{a}, \mathbf{u}(1) = \mathbf{b}$, and set $z(t) = u^1(t) + \mathbf{i}u^2(t)$. Then

$$E_1(\mathbf{u}) = \int_0^1 |z'(\tau)||z^3(\tau) - 1|\, d\tau = \int_0^1 \left|\frac{d}{d\tau}g(z(\tau))\right| d\tau = \int_0^1 |w'(\tau)|\, d\tau$$

where $w = g(z) = z - z^4/4$. Minimizing E_1 over the set of curves connecting $\mathbf{a}$ to $\mathbf{b}$ reduces to the simple problem of minimizing the length functional on the w plane, for curves connecting $g(\mathbf{a}) = 3/4$ and $g(\mathbf{b}) = 3e^{2\pi\mathbf{i}/3}/4$. This of course is minimized by the line segment connecting the image points. We can choose the following simple parametrization for the line segment:

$$g(z(\tau)) = \tau g(\mathbf{a}) + (1-\tau)g(\mathbf{b}) = \tfrac{3}{4}\{\tau + (1-\tau)e^{2\pi i/3}\}, \qquad 0 \leqslant \tau \leqslant 1.$$

It is then straightforward to show that the curve $z(\tau) = r(\tau)e^{i\theta(\tau)}$ satisfies the parameter-free equation

$$4r\cos(\theta - \pi/3) = r^4\cos(4\theta - \pi/3) + 3\cos(\pi/3), \qquad 0 \leqslant \theta \leqslant \pi/3, 0 < r < 1. \tag{1.6}$$

Following [34] we obtain the desired solution $\mathbf{u} = (\mathrm{Re}(U), \mathrm{Im}(U))$ of (1.1) by defining

https://doi.org/10.1017/S095679250600667X Published online by Cambridge University Press

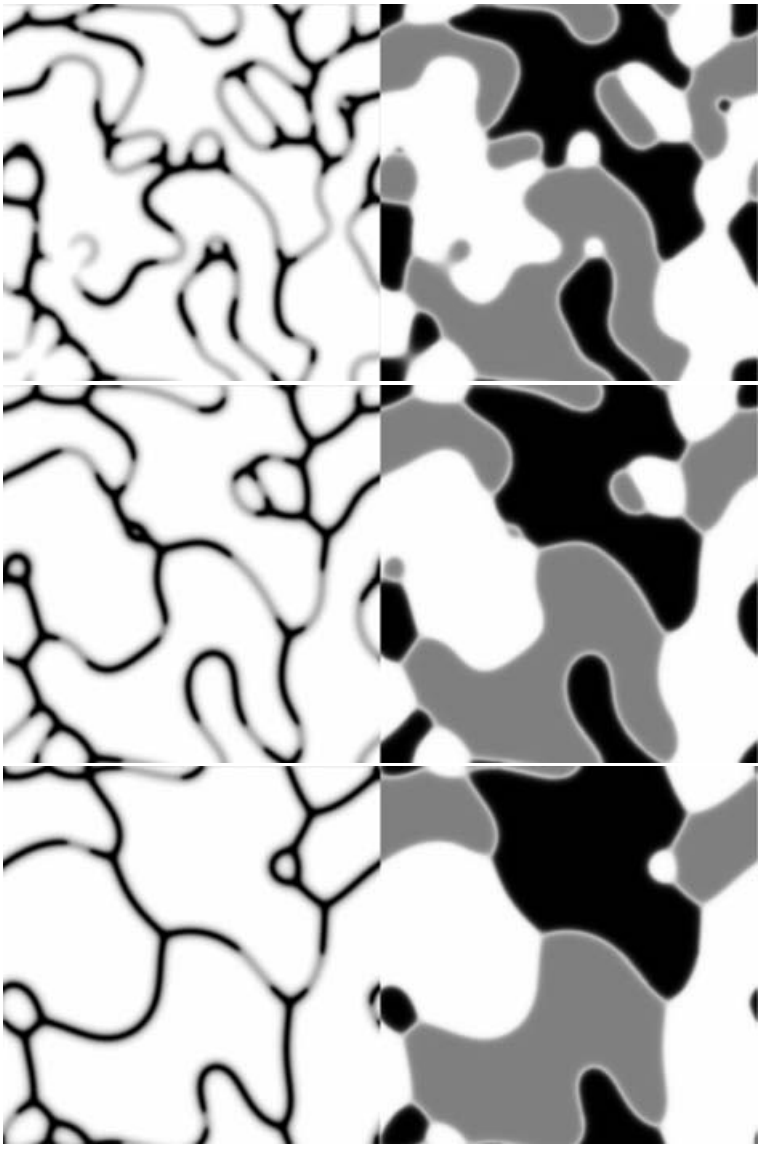

FIGURE 1. The solution of the time-dependent Allen–Cahn equations, at three different stages of the evolution. On the left of each image we show the two kinds of interfaces designated by black and grey. On the right column, each image shows three different phases corresponding to the three global minima of the potential. We caution the reader that the greyscale near or at the core of the triple junctions has no significance.

$t : \mathbb{R} \to (0, 1)$ and $U : \mathbb{R} \to \mathbb{R}^2$ via

$$U(x) = z(t(x)), \qquad \frac{dt}{dx} = \frac{\sqrt{W(z(t))}}{|z'(t)|}, \qquad t(0) = 1/2.$$

Some explanations are needed to clarify the apparent arbitrariness of the parametrizations employed above. First, we note that if one chooses to parametrize the line segment

https://doi.org/10.1017/S095679250600667X Published online by Cambridge University Press

connecting $g(\mathbf{a})$ and $g(\mathbf{b})$ in some different way, then by following through the steps one discovers that the newly obtained $\mathbf{u}(x)$ differs from the one given above only by a translation in x. Notice that the parametrization in x has the important property

$$|\mathbf{u}_x|^2 = W(\mathbf{u});$$

we call it the **equipartition parametrization**. The other distinguished parametrization is obtained by setting $s = |g(\alpha) - g(\beta)|\tau$, which satisfies $\sqrt{W(\mathbf{u})}|\mathbf{u}_s| = 1$; it is called the **arclength parametrization**.

This paper is organized as follows. In § 2, we discuss the parametrizations of a connection and alternative representations of the energy functional E in (1.2). In § 3, we present our theory on the explicit construction of connections for type I and type II potentials. This theory is generalized in § 4 to equation (1.4). We provide a number of examples for type I and type II potentials in §§ 5 and 6, respectively. Finally in § 7 we describe our numerical schemes and results for the evolution equation (1.3).

2 Equipartition and arclength parameters

One way to reduce the order of the problem is by utilizing a first integral which in our case is available since (1.1) is an equation that does not depend explicitly on x. In fact, utilizing a first integral for (1.1) we obtain the following:

Lemma 2.1 (Equipartition of energy). *Any solution* $\mathbf{u}(\cdot)$ *to (1.1) satisfies*

$$|\mathbf{u}_x|^2 = W(\mathbf{u}) \quad \textit{on} \quad \mathbb{R}, \qquad E(\mathbf{u}) = E_1(\mathbf{u}) = E_2(\Gamma(\mathbf{u}))$$

where $\Gamma(\mathbf{u}) = \{\mathbf{u}(x) \mid x \in \mathbb{R}\}$ *is the trajectory (or connection),*

$$E_1(\mathbf{u}) := \int_{\mathbb{R}} \left|\sqrt{W(\mathbf{u})}\,\mathbf{u}_x\right| dx, \qquad E_2(\gamma) := \int_{\gamma} \sqrt{W(\mathbf{u})}\ |d\mathbf{u}|.$$

Proof Let $\mathbf{u}$ solve (1.1). Then,

$$[|\mathbf{u}_x|^2 - W(\mathbf{u})]_x = 2\mathbf{u}_{xx} \cdot \mathbf{u}_x - W_{\mathbf{u}} \cdot \mathbf{u}_x = 0 \quad \text{in} \quad \mathbb{R}.$$

Hence, $|\mathbf{u}_x|^2 - W(\mathbf{u})$ is a constant function. Utilizing the limit, as $x \to -\infty$, of $\mathbf{u}$, we see that $|\mathbf{u}_x|^2 - W(\mathbf{u}) \equiv 0$. Consequently, $|\mathbf{u}_x|^2 + W(\mathbf{u}) = 2|\mathbf{u}_x\sqrt{W(\mathbf{u})}|$ and $E(\mathbf{u}) = E_1(\mathbf{u}) = E_2(\Gamma(\mathbf{u}))$. □

If $\mathbb{R}^N \setminus A$ is equipped with the metric

$$(d\ell)^2 = \sqrt{W(u)}\delta_{ij}du^i du^j,$$

it becomes a Riemannian metric space and $E_2(\gamma)$ is the length of the curve γ under the metric. This is a well known fact in Classical Mechanics [6]. In the context if interfaces, see

https://doi.org/10.1017/S095679250600667X Published online by Cambridge University Press

[34]. Since the arclength of a curve is independent of parametrization, E_2 is invariant under the change of parameters. Given a curve, we are interested in two special parameters.

Definition 1. (1) The *trajectory* of a function $\mathbf{u} : t \in (a,b) \to \mathbb{R}^N$ is the set

$$\mathbf{u}((a,b)) := \{\mathbf{u}(t) \,|\, t \in (a,b)\}.$$

(2) Let γ be a smooth curve in $\mathbb{R}^N \setminus A$. A *parametrization* of γ is a function $\mathbf{u} : t \in (a,b) \to \mathbb{R}^N$ such that $|\mathbf{u}_t| > 0$ on (a,b) and $\gamma = \mathbf{u}((a,b))$.

The parameter t is called an *equipartition* parameter if $|\mathbf{u}_t|^2 = W(\mathbf{u})$ for all $t \in (a,b)$.

It is called an *arclength parameter* (under the $\sqrt{W(\mathbf{u})}\delta_{ij}$ metric) if $\sqrt{W(\mathbf{u})}|\mathbf{u}_t| = 1$.

Here a, b may be chosen differently in (1) and in (2). The domain of the arclength parameter will always be finite while the domain of the equipartition parameter may be $(-\infty, \infty)$.

Proposition 1. [6, 34] Any smooth curve on $\mathbb{R}^N \setminus A$ admits both an equipartition parameter and an arclength parameter. All three energy functionals E, E_1, E_2 are equivalent in the following sense:

(1) E_1 and E_2 are equal if functions are related to their trajectories and curves are related to their parameterizations.

(2) For every $\mathbf{u} : \mathbb{R} \to \mathbb{R}^N$, $E(\mathbf{u}) \geqslant E_1(\mathbf{u}) = E_2(\Gamma(\mathbf{u}))$; for every (smooth) curve γ in $\mathbb{R}^N$, there is a parametrization $\mathbf{u}(\cdot)$ such that $\gamma = \Gamma(\mathbf{u})$ and $E(\mathbf{u}) = E_1(\mathbf{u}) = E_2(\gamma)$.

Proof We need only show the existence of the two parameterizations. Let γ be a smooth curve in the phase space. Here smooth means that γ can be parametrized by a smooth function $\mathbf{u} : t \in (a,b) \to \mathbb{R}^N$. Fix $c \in (a,b)$. Define

$$x(t) = \int_c^t \frac{|\mathbf{u}_t(t)|}{\sqrt{W(\mathbf{u}(t))}}\, dt, \qquad s(t) = \int_c^t \sqrt{W(\mathbf{u}(\tau))}|\mathbf{u}_t(\tau)|\, d\tau.$$

Then $\frac{dx}{dt} = |\mathbf{u}_t|/\sqrt{W(\mathbf{u})}$ and $\frac{ds}{dt} = \sqrt{W(\mathbf{u})}|\mathbf{u}_t|$. For the new parameters x and s,

$$\left|\frac{d\mathbf{u}}{dx}\right|^2 = \left|\frac{d\mathbf{u}}{dt}\,\frac{dt}{dx}\right|^2 = W(\mathbf{u}), \qquad \sqrt{W(\mathbf{u})}\left|\frac{d\mathbf{u}}{ds}\right| = \sqrt{W(\mathbf{u})}\left|\frac{d\mathbf{u}}{dt}\,\frac{dt}{ds}\right| = 1.$$

Thus, x is an equipartition parameter and s is an arclength parameter. □

3 Expressing trajectories in closed form

In the sequel, we shall focus our attention to the case $N = 2$. Hence we identify $\mathbb{R}^2$ with the complex plane $\mathbb{C}$, and identify $\mathbf{u} = (u^1, u^2)$ with the complex number $z = u^1 + \mathbf{i}u^2$. Similarly, we write $W(\mathbf{u})$ as $W(z)$. Since $W(\cdot)$ is non-negative, we can write $W(z) = |f(z)|^2$ for some f. From now on we focus our attention to the case that f is analytic. It is easy to verify that the equation $2\mathbf{u}_{xx} = W_{\mathbf{u}}(\mathbf{u})$ is equivalent to

$$z_{xx} = f(z)\overline{f'(z)} \tag{3.1}$$

https://doi.org/10.1017/S095679250600667X Published online by Cambridge University Press

where the bar represents complex conjugation and f' the derivative of f. We use $\mathrm{Im}(z)$, $\mathrm{Re}(z)$, and $\mathrm{Arg}(z)$ to denote the imaginary part, real part, and argument of a complex number z, respectively.

Theorem 1 *Identify the point (u^1, u^2) with the complex number $z = u^1 + \mathbf{i}u^2$ and write $W(u^1, u^2) = |f(z)|^2$. Assume that $f = g'$ is holomorphic in D, an open set in $\mathbb{R}^2$. Let $\gamma = \{\mathbf{u}(x) \mid x \in (a, b)\}$ be a smooth curve in D where x is an equipartition parameter, i.e. $|\mathbf{u}_x|^2 = |W(\mathbf{u})|$. Set $\alpha = \mathbf{u}(a)$, $\beta = \mathbf{u}(b)$.*

Then $\mathbf{u}$ is a solution to $2\mathbf{u}_{xx} = W_{\mathbf{u}}(\mathbf{u})$ on (a, b) if and only if

$$\mathrm{Im}\Big(\frac{g(z) - g(\alpha)}{g(\beta) - g(\alpha)}\Big) = 0 \quad \forall\, z \in \gamma. \tag{3.2}$$

In addition, in the case of $\mathbf{u}$ being a solution, the set $g(\gamma) := \{g(z) \mid z \in \gamma\}$ is a line segment with end points $g(\alpha)$ and $g(\beta)$ and the (partial) transition energy is given by

$$\tfrac{1}{2}\int_a^y \Big(|\mathbf{u}_x|^2 + W(\mathbf{u})\Big)dx = \int_a^y \Big|\frac{d}{dx}\, g(\mathbf{u})\Big|dx = |g(\mathbf{u}(y)) - g(\alpha)| \quad \forall y \in (a, b]. \tag{3.3}$$

This theorem states in geometric terms that geodesics in the $\sqrt{W(u)}\delta_{ij}$ metric are mapped under g to straight line segments in the complex plane. This is the essence of the calculation at the end of the introduction.

The theorem implies the following:

(i) A trajectory to (1.1) satisfies the parameter free equation (3.2), for some $\alpha, \beta \in A$.

(ii) An equipartition parametrization of any curve satisfying (3.2) is a solution to $2\mathbf{u}_{xx} = W_{\mathbf{u}}(\mathbf{u})$.

(iii) The energy of a connection is the magnitude of the difference of g between the end points.

Proof ("$\Rightarrow$") Suppose $\mathbf{u} = (u^1, u^2) : (a, b) \to D$ is a solution to

$$2\mathbf{u}_{xx} = W_{\mathbf{u}}(\mathbf{u}), \qquad |\mathbf{u}_x|^2 = W(\mathbf{u}).$$

Set $z(x) = u^1(x) + \mathbf{i}u^2(x)$. Then $z_{xx} = f(z)\overline{f'(z)}$ and $|z_x|^2 = f(z)\overline{f(z)}$.

Let L be the total arclength and ℓ be the arclength parameter defined by

$$L = \int_a^b |\mathbf{u}_x|\, \sqrt{W(\mathbf{u})}\, dx, \quad \ell = \int_a^x |\mathbf{u}_x(\hat{x})|\, \sqrt{W(\mathbf{u}(\hat{x}))}\, d\hat{x}.$$

Then $\frac{d}{d\ell} = (\sqrt{W(\mathbf{u})}|\mathbf{u}_x|)^{-1}\frac{d}{dx} = (f\bar{f})^{-1}\frac{d}{dx}$, so that

$$\frac{dg(z)}{d\ell} = \frac{g'(z)z_x}{f(z)\overline{f(z)}} = \frac{f(z)z_x}{f(z)\overline{f(z)}} = \frac{z_x}{\bar{f}},$$

$$\frac{d^2g(z)}{d\ell^2} = \frac{\bar{f}\, z_{xx} - z_x\overline{f'}\, \overline{z_x}}{\bar{f}^2\, f\, \bar{f}} = \frac{\bar{f}\, z_{xx} - |z_x|^2\overline{f'}}{f\bar{f}^3} = \frac{z_{xx} - f\overline{f'}}{f\bar{f}^2} = 0.$$

Thus, $\frac{d}{d\ell}g(z) = m$ is a constant.[1]

[1] If $m = 0$ it follows that $g(z(t)) = g(\alpha)$, and since g is analytic $z(t) = \alpha$. Thus, if $u(x)$ is a heteroclinic it follows that $m \neq 0$ and so $g(z_i) \neq g(z_j)$.

https://doi.org/10.1017/S095679250600667X Published online by Cambridge University Press

Integrating this equation and evaluating it at $\ell = L$ gives, respectively, $g(z) = g(\alpha) + m\ell$ and $mL = g(\beta) - g(\alpha)$. Upon noting that $m = \frac{d}{d\ell} g(z) = z_x / \overline{f(z)}$ has unit length, we then obtain

$$L = |g(\beta) - g(\alpha)|, \quad m = \frac{g(\beta) - g(\alpha)}{|g(\beta) - g(\alpha)|}, \qquad g(z(\ell)) = \frac{L - \ell}{L} g(\alpha) + \frac{\ell}{L} g(\beta).$$

These equations imply (3.2) and (3.3).

("$\Leftarrow$") Next assume that $\gamma = \mathbf{u}((a, b))$ satisfies (3.2) and the parameter x for $\mathbf{u}$ is an equipartition parameter, namely, $|\mathbf{u}_x|^2 = W(\mathbf{u})$. Equation (3.2) can be written as

$$g(z) - g(\alpha) = s(x)(g(\beta) - g(\alpha))$$

where $s(\cdot)$ is a real valued function. Upon differentiation, we obtain

$$s_x(g(\beta) - g(\alpha)) = g'(z) z_x = f(z) z_x.$$

This equation implies that $|s_x| = \frac{|f(z)||z_x|}{|g(\beta) - g(\alpha)|} = \frac{|f(z)|^2}{|g(\beta) - g(\alpha)|} > 0$. As $s(x)$ is a real valued function, $s(a) = 0$ and $s(b) = 1$, we must have $s_x(x) > 0$. Hence, $s_x(x) = \frac{|f(z)|^2}{|g(\beta) - g(\alpha)|}$. Consequently,

$$z_x = \frac{s_x(g(\beta) - g(\alpha))}{f(z)} = \frac{|f(z)|^2 (g(\beta) - g(\alpha))}{f(z)|g(\beta) - g(\alpha)|} = m\overline{f(z)}$$

where $m = \frac{g(\beta) - g(\alpha)}{|g(\beta) - g(\alpha)|}$. Thus,

$$z_{xx} = m\overline{f'(z) z_x} = m\overline{f'(z) m \overline{f(z)}} = |m|^2 f \overline{f'} = f(z)\overline{f'(z)}.$$

This equation is equivalent to $\mathbf{u}$ being a solution to $2\mathbf{u}_{xx} = W_{\mathbf{u}}(\mathbf{u})$. □

Remark 3.1 (1) The proof implies that (1.1) is equivalent to the first order ode:

$$z_x = m\overline{f(z)}, \qquad m \in \mathbb{C}, \quad |m| = 1. \tag{3.4}$$

(2) Multiplying (3.4) by $f(z)/m$ gives

$$\frac{d}{dx} \frac{g(z)}{m} = |f(z)|^2 = W > 0.$$

Integrating this equation gives

$$\mathrm{Im}\left(\frac{g(z) - g(\alpha)}{m} \right) = 0, \quad \frac{g(z) - g(\alpha)}{m} = \int_a^x W(z(\hat{x}))\, d\hat{x} = \ell.$$

This in particular implies that the map $x \to g((z(x))$ is a one-to-one map.

(3) We will be applying the theorem above to the solutions of (1.1) connecting at infinity two wells, thus we would like to take $(a, b) = (-\infty, \infty)$. The question then is whether $L = E_1(\mathbf{u}) = \int_{-\infty}^{\infty} |u_x| \sqrt{W(u)}\, dx$ is finite. Certainly, this is the case if the matrices $W_{\mathbf{uu}}(\mathbf{u}(\pm\infty))$ are non-degenerate (i.e. $det(W_{\mathbf{uu}}) \neq 0$), since then by standard linear ODE theory the convergence of $\mathbf{u}(\mathbf{x})$ to $\mathbf{u}(\pm\infty)$ is exponential and $|\mathbf{u}_x|$ decays exponentially, so $L < \infty$.

https://doi.org/10.1017/S095679250600667X Published online by Cambridge University Press

(4) The assumption that x in Theorem **1** is an equipartition parameter is in a sense superfluous since any solution to (1.1) satisfies the equipartition identity and any curve admits an equipartition parametrization.

As an important application of the above theorem, we can show the following.

Theorem 2 *There exists at most one trajectory connecting any two wells of a holomorphic potential; that is, if $W(z) = |f(z)|^2$ where f is holomorphic on $\mathbb{C}$, there exists at most one trajectory of (1.1) that connects any two roots of $W(z) = 0$.*

Proof Let g be an antiderivative of f and suppose that γ_1 and γ_2 are two trajectories to (1.1) with the same end points α, β. Since the energy $|g(\beta) - g(\alpha)|$ is positive, $g(\beta) \neq g(\alpha)$ and we can define an entire function

$$\tilde{g}(z) = \frac{|g(\beta) - g(\alpha)|}{g(\beta) - g(\alpha)}(g(z) - g(\alpha)) \qquad \forall z \in \mathbb{C}.$$

Then $\tilde{g}$ is real on $\gamma_1 \cup \gamma_2$. Now if $\gamma_1 \neq \gamma_2$, then γ_1 and γ_2 will enclose an open domain D in $\mathbb{C}$. As the imaginary part of $\tilde{g}$ on $\partial D = \gamma_1 \cup \gamma_2 \cup \{\alpha, \beta\}$ is zero, it has to be identically zero in D. This implies that $\tilde{g}$ is a constant function in $\mathbb{C}$ which is impossible. Thus $\gamma_1 = \gamma_2$. □

To construct potentials having multiple connections between roots of zeros, we use meromorphic potentials. For these potentials, their antiderivative may have branches. For this purpose, we extend our Theorem **1** as follows:

Theorem 3 *Assume that $W(z) = |f(z)|^2$ where f is meromorphic in an open domain D. Let D_i, $i = 1, \ldots, k$, be a family of overlapping subdomains of D in the sense that $D_i \cap D_{i+1} \neq \emptyset$ for $i = 1, \ldots, k-1$. Let g_i be an antiderivative of f in D_i. Assume that g_{i+1} is an analytic extension of g_i in the sense that $g_{i+1} = g_i$ on $D_i \cap D_{i+1} \neq \emptyset$.*

Let γ be a smooth curve in D with parametrization $z = z(t)$, $t \in (a, b)$. Assume that $z((a_i, b_i)) \subset D_i$ and $(a, b) = \cup_{i=1}^{k}(a_i, b_i)$ where $a_1 = a$, $b_k = b$, and $a_i < a_{i+1} < b_i < b_{i+1}$. Then $z((a, b))$ is a trajectory to (1.1) if and only if $\cup_{i=1}^{k} g_i(z(a_i, b_i))$ is a line segment, or equivalently, if and only if

$$\operatorname{Im}\left(\frac{g_i(z(t)) - g_1(z(a))}{g_i(z(b)) - g_1(z(a))}\right) = 0 \qquad \forall t \in (a_i, b_i), \quad i = 1, \ldots, k. \tag{3.5}$$

In addition, in case γ is a trajectory, its total energy is given by $|g_k(z(b)) - g_1(z(a))|$.

Proof Since g_{i+1} is an analytic extension of g_i, the function $h : (a, b) \to \mathbb{C}$ given by

$$h(t) = g_i(z(t)) \quad \text{if} \quad t \in (a_i, b_i)$$

is well-defined and is a smooth function on (a, b).

https://doi.org/10.1017/S095679250600667X Published online by Cambridge University Press

Suppose γ is a trajectory to (3.1). Since $g_i' = f$ in D_i and $h(t) = g_i(z(t))$ for $t \in (a_i, b_i)$, $h((a_i, b_i))$ is a line segment and the map $t \in (a_i, b_i) \to h(t)$ is a one-to-one map. Thus, $h((a, b))$ is a line segment with end points $h(a) = g_1(z(a))$ and $h(b) = g_k(z(b))$.

On the other hand, if (3.5) holds, then $z((a_i, b_i))$ is a trajectory of (3.1) for each $i = 1, \ldots, k$, and therefore $\gamma = z((a, b))$ is also a trajectory of (3.1). □

Remark 3.2 The feature of the potential with poles is that it is multivalued and that paths on the complex plane connecting two wells lie on distinct Riemann surfaces.

4 An extension

Given a constant $p > 1$, define

$$E_p(\mathbf{u}) := \int_{\mathbb{R}} \left(\frac{|\mathbf{u}_x|^p}{p} + \frac{W(\mathbf{u})}{q} \right) dx, \qquad \frac{1}{p} + \frac{1}{q} = 1.$$

By Young's inequality, $\alpha\beta \leqslant |\alpha|^p/p + |\beta|^q/q$,

$$E_p(\mathbf{u}) \geqslant E_{1p}(\mathbf{u}) := \int_{\mathbb{R}} |\mathbf{u}_x| \sqrt[q]{W(\mathbf{u})}\, dx = \int_{\Gamma(\mathbf{u})} \sqrt[q]{W(\mathbf{u})}\, |d\mathbf{u}|.$$

Note that the second expression of E_{1p} is in parametric form.

The Euler-Lagrange equation associated with E_p is

$$q \left(|\mathbf{u}_x|^{p-2} \mathbf{u}_x \right)_x = W_{\mathbf{u}}(\mathbf{u}) \tag{4.1}$$

which together with the conditions $\lim_{|x| \to \infty} W(\mathbf{u}(x)) = 0$ constitutes the analog to (1.1). The analogous energy equipartition relationship is

$$|\mathbf{u}_x|^p = W(\mathbf{u}) \quad \Longleftrightarrow \quad E_p(\mathbf{u}) = E_{1p}(\mathbf{u}).$$

The potentials are those of the form

$$W(u, v) = |f(z)|^q, \ z = u + iv,$$

where $f(z)$ is analytic, or analytic modulo poles. For example the analog of the standard triple-well potential in this context is

$$W(z) = |z^3 - 1|^q.$$

Comparing with the method presented in the introduction for $|z^3 - 1|^2$ we see that the minimizer on the transformed plane is again a line segment, and the trajectory is exactly the same as before, given by (1.6), being independent of p. The dependence on p is through the parametrization

$$\frac{dt}{dx} = \frac{\sqrt[q]{W(z(t))}}{|z'(t)|}, \qquad t(0) = 1/2$$

https://doi.org/10.1017/S095679250600667X Published online by Cambridge University Press

which leads to the connection $\mathbf{u}(x) = z(t(x))$. We expect that all the results in this paper extend for $p > 1$.

The analog of the vector Allen–Cahn equation is (1.5).

5 Examples of entire potentials

In this section, we provide several examples of potentials $W = |f|^2$ where f is an entire function, i.e., analytic on $\mathbb{C}$. We remark that if we are working with equation (4.1), the only change we need is to set $W = |f|^q$.

Example 1. $W(z) = |z^n - 1|^2$ where $n \geqslant 2$ is an integer. The set A of wells is given by

$$A = \{e^{2k\mathbf{i}/n} \mid k = 0, \dots, n-1\}.$$

In this case we take

$$f(z) = 1 - z^n, \qquad g(z) = \int_0^z f(\zeta)\, d\zeta = z\Big(1 - \frac{z^n}{n+1}\Big).$$

Given two different wells $e^{2k\pi\mathbf{i}/n}$ and $e^{2l\pi\mathbf{i}/n}$, a trajectory to (1.1) is determined by the preimage under g of the line segment connecting $g(e^{2k\pi\mathbf{i}/n})$ and $g(e^{2l\pi\mathbf{i}/n})$. This amounts to finding $z(t)$, for each t, from the equation

$$z\Big(1 - \frac{z^n}{n+1}\Big) = \frac{n}{n+1}\Big(te^{2k\pi\mathbf{i}/n} + (1-t)e^{2l\pi\mathbf{i}/n}\Big), \quad t \in (0,1). \tag{5.1}$$

We observe the following:

(i) Restricted to the closed disk $D = \{z \in \mathbb{C} \mid |z| \leqslant 1\}$, the map g is one-to-one.
(ii) $\min_{|z|=1} |g(z)| = \frac{n}{n+1}$; hence $g(D)$ contains the disk $\{w \in \mathbb{C} \mid |w| \leqslant \frac{n}{n+1}\}$.
(iii) The right-hand side of (5.1) is contained in the disk $\{w \in \mathbb{C} \mid |w| \leqslant \frac{n}{n+1}\}$.

Thus, equation (5.1) is uniquely solvable in D. By the uniqueness, we thus know that the solution in D to (5.1) provides the needed trajectory. In terms of the polar coordinates $z = re^{\mathbf{i}\theta}$, (5.1) with $|z| \leqslant 1$ can be written in the non-parametric form

$$\begin{cases} (n+1)r\cos\Big(\theta - \frac{k+l}{n}\pi\Big) = r^{n+1}\cos\Big((n+1)\theta - \frac{k+l}{n}\pi\Big) + n\cos\Big(\frac{k-l}{n}\pi\Big), \\ \frac{k\pi}{n} \leqslant \theta \leqslant \frac{l\pi}{n}, \qquad 0 < r \leqslant 1. \end{cases} \tag{5.2}$$

In conclusion, we have the following.

Proposition 5.1 *Suppose $W(z) = |z^n - 1|^2$ where $n \geqslant 2$ is an integer. For each pair of roots of $W = 0$, there exists exactly one trajectory of* (1.1) *that connects the two roots. The energy of the connection between $e^{2k\pi\mathbf{i}/n}$ and $e^{2l\pi/n}$, l,k integers, is given by*

$$\frac{2n}{n+1}\Big|\sin\frac{k-l}{n}\pi\Big|.$$

https://doi.org/10.1017/S095679250600667X Published online by Cambridge University Press

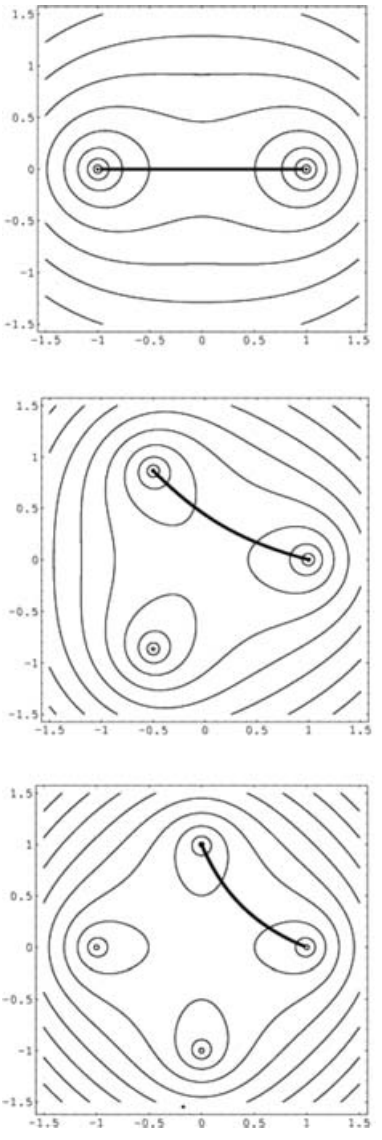

FIGURE 2. Trajectories and level sets of W for Example **1** with $n = 2, 3$, and 4 respectively. For $n = 4$ there are also vertical and horizontal lines representing trajectories connecting the wells, that are not shown above.

Moreover the trajectory is given in non-parametric closed form by (5.2) *or alternatively in parametric form by the solutions to* (5.1) *in the unit disk.*

Example 2. $W(z) = |(1 - z^2)(z^2 + \varepsilon^2)|^2,\ 0 < \varepsilon < \infty.$

In this case, we can take

$$f(z) = (1 - z^2)(z^2 + \varepsilon^2), \qquad g(z) = z(\varepsilon^2 + \tfrac{1}{3}(1 - \varepsilon^2)z^2 - \tfrac{1}{5}z^4),$$
$$g(\pm 1) = \pm(\tfrac{2}{3}\varepsilon^2 + \tfrac{2}{15}), \qquad g(\pm \mathbf{i}\varepsilon) = \pm \mathbf{i}\varepsilon^3(\tfrac{2}{3} + \tfrac{2}{15}\varepsilon^2).$$

https://doi.org/10.1017/S095679250600667X Published online by Cambridge University Press

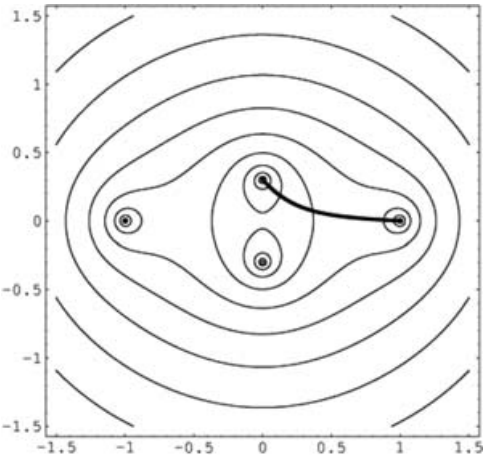

FIGURE 3. A trajectory in Example **2** for $\varepsilon = 0.3$. The other two connections are horizontal and vertical straight line segments connecting the wells.

(i) Since $g(t)$, $t \in [-1,1]$ is monotone, $g([-1,1]) = [g(-1), g(1)], g^{-1}([g(-1), g(1)]) = [-1,1]$, the line segment $[-1,1]$ is the trajectory of (1.1) connecting $-1, 1$.

(ii) Since $\mathbf{i}g(\mathbf{i}t)$, $t \in (-\varepsilon, \varepsilon)$, is monotone, the line segment joining $-\mathbf{i}\varepsilon$ and $\mathbf{i}\varepsilon$ is the trajectory of (1.1) connecting $-\mathbf{i}\varepsilon$ and $\mathbf{i}\varepsilon$.

(iii) By checking the boundary behavior of g on the square $[0,1] \times [0,\varepsilon]$, one can see that there is a connection from 1 to $\mathbf{i}\varepsilon$ lying entirely in the square $[0,1] \times [0,\varepsilon]$. By symmetry, we can obtain connections from ± 1 to $\pm\mathbf{i}\varepsilon$.

In conclusion, between each pair of wells of W, there is a unique connection.

In the above two examples, there is always a connection between each pair of wells. Next we provide an example where certain wells may not be connected.

Example 3. $W(z) = |(1-z^2)(z-\mathbf{i}\varepsilon)|^2$, $0 \leqslant \varepsilon < \infty$.
In this case we take

$$f(z) := \mathbf{i}(1-z^2)(z-\mathbf{i}\varepsilon),\ \ g(z) = \varepsilon z(1-\tfrac{1}{3}z^2) - \frac{1}{4}\mathbf{i}(z^2-1)^2.$$

$$g(\pm 1) = \pm\tfrac{2}{3}\varepsilon,\ \ g(\mathbf{i}\varepsilon) = \frac{\mathbf{i}}{12}(\varepsilon^4 + 6\varepsilon^2 - 3).$$

It is not very hard to show that there is a connection between ± 1 and $\mathbf{i}\varepsilon$. Now we investigate the possibility of existence of a connection from -1 to 1. By a simple comparison of $|g(1) - g(-1)|$ with $|g(1) - g(\mathbf{i}\varepsilon)|$ it is expected that there is no connection between 1 and -1 when ε is small and there is a connection when ε is large. More precisely we see that for $\varepsilon > 0$ (and small), $|g(1) - g(0)| = 4\varepsilon/3$, $(|g(i\varepsilon) - g(1)| \sim 1/4)$. If there is a connection between -1 and 1 then its energy by Theorem 1 should equal $\sqrt{2}|g(1) - g(-1)| = 4\sqrt{2}\varepsilon/3$. It is unlikely that this energy would be sufficient for connecting two points a fixed distance away if ε is very small. This is the intuition behind this example.

https://doi.org/10.1017/S095679250600667X Published online by Cambridge University Press

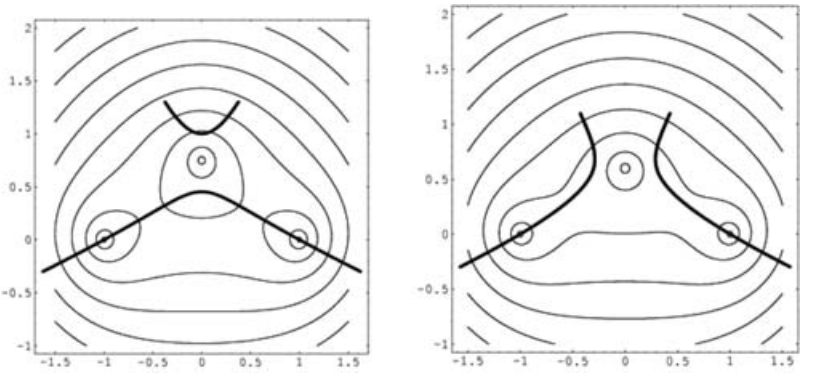

FIGURE 4. Trajectories in Example **3** with two values of ε, one ($= 0.75$) slightly above and the other ($= 0.6$) slightly below the critical value ($= 0.68\ldots$).

.

Here we would like to find the critical ε. The issue in this example is the non-invertibility of g.

Suppose there is a connection γ between -1 and 1. Then γ has to intersect the imaginary axis, say at $\mathbf{i}t$ where $t \in \mathbb{R}$. Since $g(\gamma)$ is the line segment $[-\frac{2}{3}\varepsilon, \frac{2}{3}\varepsilon]$, $g(\mathbf{i}t) = \mathbf{i}(\varepsilon t(1 + \frac{1}{3}t^2) - \frac{1}{4}(1 + t^2)^2)$ must be real. Hence,

$$\varepsilon t(1 + \tfrac{1}{3}t^2) - \tfrac{1}{4}(1 + t^2)^2 = 0.$$

The left-hand side, as a function of the real variable t, attains its maximum at $t = \varepsilon$ with value

$$\tfrac{1}{12}(\varepsilon^4 + 6\varepsilon^2 - 3).$$

Hence, when the above quantity is non-positive, e.g. $\varepsilon^2 \leqslant 2\sqrt{3} - 3$, there is no connection between -1 to 1. On the other-hand, when $\varepsilon^2 > 2\sqrt{3} - 3$, $g(\mathbf{i}t) = 0$ has exactly two positive roots t_1, t_2 where $0 < t_1 < \varepsilon < t_2$. In this case, one can show that the preimage under g of $[-\frac{2}{3}\varepsilon, \frac{2}{3}\varepsilon]$ contains a smooth curve joining -1,1 that goes through $\mathbf{i}t_1$. This curve is the trajectory connecting -1 and 1. We summarize our result as follows.

Proposition 5.2 *Let* $W(z) = |(z^2 - 1)(z - \mathbf{i}\varepsilon)|^2$ *where* $\varepsilon \in \mathbb{R}$. *Then the dynamics (1.1) admits a connection between* -1 *and* 1 *if and only if* $|\varepsilon| > \sqrt{2\sqrt{3} - 3} = 0.68125\ldots$

6 Singular potentials

As demonstrated in Theorem 2, for holomorphic potentials, there exists at most one connection between any given pair of wells. To construct examples of multiple connections, we shift our attention to potentials with poles. We work only on (1.1) so $W = |f|^2$. For (4.1), the only change needed is to set $W = |f|^q$. We remark that since the connections do not go through the pole, the potential can be smoothened out near the pole without affecting the connection hence rendering examples of C^∞ potentials with non-uniqueness of the connections.

https://doi.org/10.1017/S095679250600667X Published online by Cambridge University Press

Example 4. $W(z) = |(z-1)(z+a)/z|^2,\ 0 < a < 1.$
We take

$$f(z) = z + (a-1) - \frac{a}{z}, \qquad g(z) = \tfrac{1}{2}(z^2-1) + (a-1)(z+1) - a\log z.$$

To find all possible connections, we use the Riemann surface by defining

$$z = re^{\mathbf{i}\theta}, \quad \log z = \ln r + \mathbf{i}\theta \quad \forall\, r \in (0,\infty), \theta \in (-\infty,\infty).$$

We seek a connection from $b := e^{0\mathbf{i}}$ to $a_k := ae^{(2k+1)\pi\mathbf{i}}$ where k is an integer. This amounts to finding a smooth curve $z_k(t), 0 \leqslant t \leqslant 1$ such that $z_k(1) = ae^{(2k+1)\pi\mathbf{i}}$, and

$$z_k(0) = e^{0\mathbf{i}}, \qquad g(z_k(t)) = tg(ae^{(2k+1)\pi\mathbf{i}}) + (1-t)g(e^{0\mathbf{i}}) \ \ \forall\, t \in (0,1]. \tag{6.1}$$

Let k be fixed. We use the Taylor expansion $g(z) \sim g(e^{0\mathbf{i}}) + \frac{1}{2}(1+a)(z-1)^2$ to conclude that for small positive t, (6.1) admits exactly two solutions, $z_k^+(t)$, on the upper-half plane, and $z_k^-(t)$, on the lower half plane.

Next, we follow the path of z_k^+. By the implicit function theorem, $z_k^+(\cdot)$ can be locally uniquely extended as long as $g'(z_k^+(t)) = f(z_k^+(t)) \neq 0$. Since $\{tg(ae^{(2k+1)\pi\mathbf{i}}) + (1-t)g(e^{0\mathbf{i}}) \mid t \in (0,1)\}$ is bounded and has an empty intersection with the set $\{g(e^{2l\pi\mathbf{i}}), g(ae^{(2m+1)\pi\mathbf{i}})\}_{l,m=-\infty}^{\infty}$, $z_k^+(\cdot)$ can be uniquely extended for all $t \in (0,1)$. We now determine $z_k^+(1) = \lim_{t\nearrow 1} z_k^+(t)$.

Consider the map g restricted on

$$D^+ = \{re^{\theta\mathbf{i}} \mid 0 < r < \infty, 0 < \theta < \pi\}.$$

By considering the image, under g, of the boundary of the set

$$D^+_{\varepsilon,R} = \{re^{\mathbf{i}\theta} \mid \varepsilon < r < R, 0 < \theta < \pi\}$$

and letting $\varepsilon \searrow 0$ and $R \to \infty$, one can conclude that the function g maps D in a one-to-one manner onto the whole complex plane, taking away the half line $[2(a-1),\infty)$ and the half line $-a\pi\mathbf{i} + [-\frac{1}{2}(a^2-1) - a\ln a, \infty)$. Let us denote the inverse of g restricted to D^+ by g_*^{-1}.

Since $z_k^+(t) \in D^+$ for small positive t and since $tg(ae^{(2k+1)\pi\mathbf{i}}) + (1-t)g(e^{0\mathbf{i}}) \in g(D^+)$ for all $t \in (0,1)$, we see that $z_k^+(t) \in D^+$ for all $t \in (0,1)$. In particular, $z_k^+(1) = g_*^{-1}(g(ae^{(2k+1)\pi\mathbf{i}}))$. Thus, when $k = 0$, $z_0^+(1) = ae^{\pi\mathbf{i}}$. When $k \neq 0$, $z_k^+(1) = g_*^{-1}(g(ae^{(2k+1)\pi\mathbf{i}}))$ is a complex number with a positive imaginary part, i.e. $z_k^+(1) \neq ae^{(2k+1)\pi\mathbf{i}}$; thus $z_k^+(\cdot)$ is not a connection.

Similarly, the uniquely defined $z_k^-(\cdot)$ is a connection if and only if $k = -1$.

In conclusion, we obtain the following.

Proposition 6.1 *Suppose $W(z) = |(z-1)(z+a)/z|^2$ where $a \in (0,1)$. There are exactly two connections from $-a$ to 1, one in the upper half plane and one in the lower half plane. These two connections are symmetric about the real line; see* Figure 5a.

Example 5. $W(z) = \left|\dfrac{z^2+1}{z^2-\varepsilon^2}\right|^2,\ 0 < \varepsilon < \infty.$

https://doi.org/10.1017/S095679250600667X Published online by Cambridge University Press

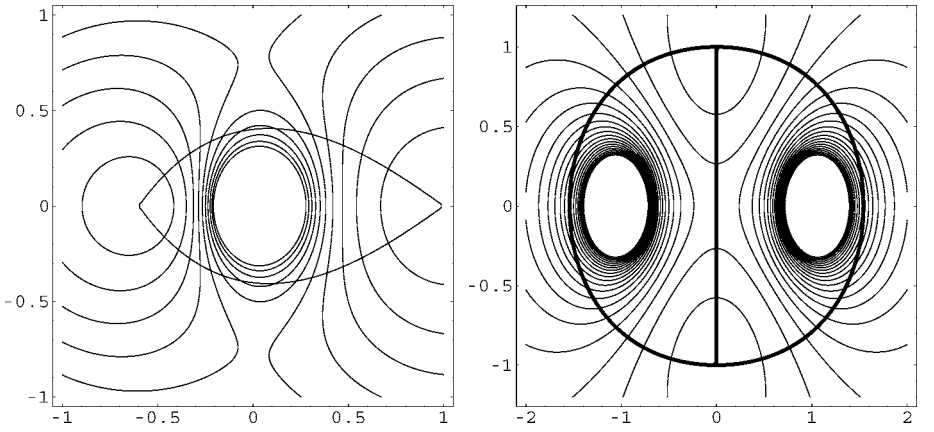

FIGURE 5. Level sets and Trajectories for Examples **4** (left) and **5** (right.)

We take

$$f(z) = \frac{z^2+1}{z^2-\varepsilon^2}, \quad g(z) = z + \frac{1+\varepsilon^2}{2\varepsilon}\log\frac{z-\varepsilon}{z+\varepsilon}.$$

We find, for integers k and l,

$$g(\mathbf{i}) = \mathbf{i} + \frac{1+\varepsilon^2}{\varepsilon}\Big(\arctan\varepsilon + k\pi\Big)\mathbf{i}, \qquad g(-\mathbf{i}) = -\mathbf{i} - \frac{1+\varepsilon^2}{\varepsilon}\Big(\arctan\varepsilon + l\pi\Big)\mathbf{i}.$$

Equation (3.2) then takes the form $\mathrm{Re}(g(z) - g(\mathbf{i})) = 0$, or writing $z = x + \mathbf{i}y$,

$$x + \frac{1+\varepsilon^2}{4\varepsilon}\ln\frac{(x-\varepsilon)^2+y^2}{(x+\varepsilon)^2+y^2} = 0.$$

This gives us three solutions. One being the line segment $\mathbf{i}[-1,1]$. The other two are the left and right halves of the curve given by

$$y^2 = 2\varepsilon x\coth\frac{2\varepsilon x}{1+\varepsilon^2} - x^2 - \varepsilon^2, \quad x \neq 0. \tag{6.2}$$

By a slightly more detailed analysis, it can be shown that the curve encloses the poles ε and $-\varepsilon$; see Figure 5b. Indeed we can have the following.

Proposition 6.2 *Let* $W(z) = \left|\dfrac{z^2+1}{z^2-\varepsilon^2}\right|^2$ *where* $0 \leqslant \varepsilon < \infty$.

(1) For $\varepsilon = 0$, *there are exactly two trajectories connecting* $-\mathbf{i}$ *and* $\mathbf{i}$, *the right and left part of the unit circle.*

(2) For $\varepsilon > 0$, *there are three trajectories* $\gamma_1, \gamma_2, \gamma_3$ *that connect* $\mathbf{i}$ *and* $-\mathbf{i}$, *where* γ_1 *is the line segment joining* $\mathbf{i}$ *and* $-\mathbf{i}$, γ_2 *is the left-half and* γ_3 *is the right-half of the curve given by (6.2).*

https://doi.org/10.1017/S095679250600667X Published online by Cambridge University Press

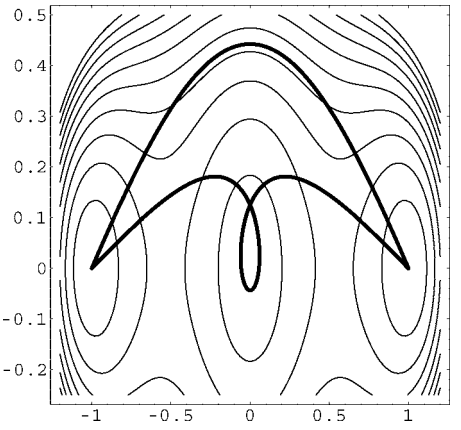

FIGURE 6. Trajectories in Example **6** with $\varepsilon = 0.2$, $k = 0$ and 1 respectively.

Their energies $E(\cdot)$ are

$$E(\gamma_1) = \frac{1+\varepsilon^2}{\varepsilon}\Big(\pi - 2\arctan\varepsilon\Big) - 2, \qquad E(\gamma_2) = E(\gamma_3) = 2 + \frac{2(1+\varepsilon^2)}{\varepsilon}\arctan\varepsilon.$$

Consequently, denote by $\varepsilon^* = 0.4416\ldots$ the unique positive solution to $\frac{\varepsilon^*}{1+\varepsilon^2} + \arctan\varepsilon^* = \frac{\pi}{4}$. Then

$$E(\gamma_2) < E(\gamma_1) \text{ when } 0 < \varepsilon < \varepsilon^*, \qquad E(\gamma_2) > E(\gamma_1) \text{ when } \varepsilon > \varepsilon^*.$$

Example 6. $W(z) = |(1-z^2)z^{\varepsilon-1}|^2$, $0 < \varepsilon < 1$.

Proposition 6.3 *Let $W(z) = |(z^2-1)z^{\varepsilon-1}|^2$ where $0 < \varepsilon < 1$. Denote by K be the largest positive integer such that $(2K-1)\varepsilon < 1$. All trajectories connecting 1 and -1 consist of K pairs, in each of which the two trajectories are symmetric about the real axis and make exactly $k+\frac{1}{2}$ loops (one clockwise, the other counterclockwise) around the origin with energy*

$$\frac{4}{\varepsilon(2+\varepsilon)}\sin\Big((k+\tfrac{1}{2})\varepsilon\pi\Big), \qquad k = 0,\ldots,K-1.$$

Proof As before, we use the Riemann surface $\mathbb{C}^* = \{re^{\mathbf{i}\theta} \mid r > 0, -\infty < \theta < \infty\}$ and set

$$z = re^{\mathbf{i}\theta}, \quad z^\varepsilon = r^\varepsilon e^{\mathbf{i}\varepsilon\theta}.$$

We can take

$$f(z) = (1-z^2)z^{\varepsilon-1}, \qquad g(z) = z^\varepsilon\Big(\frac{1}{\varepsilon} - \frac{z^2}{2+\varepsilon}\Big),$$
$$g(e^{0\mathbf{i}}) = \Big(\frac{1}{\varepsilon} - \frac{1}{2+\varepsilon}\Big), \qquad g(e^{(2k+1)\pi\mathbf{i}}) = \Big(\frac{1}{\varepsilon} - \frac{1}{2+\varepsilon}\Big)e^{(2k+1)\varepsilon\pi\mathbf{i}}.$$

We know that if γ is a trajectory connecting -1 and 1, then $g(\gamma)$ is a line segment from

https://doi.org/10.1017/S095679250600667X Published online by Cambridge University Press

$g(e^{0\mathbf{i}})$ to $g(e^{(2k+1)\pi\mathbf{i}})$ for some integer k. Using Theorem 4 we know that $\gamma = z([0,1])$ where $z(\cdot)$ is a smooth solution to $g(z(t)) = (1-t)g(e^{0\mathbf{i}}) + tg(e^{(2k+1)\pi\mathbf{i}}) \quad \forall, t \in [0,1]$. Hence, writing $z(t) = r(t)e^{i\varphi(t)}, t \in [0,1]$, we seek smooth real valued functions $r(t)$ and $\varphi(t)$ such that

$$\begin{cases} r(t)e^{\ \varepsilon\varphi(t)\mathbf{i}}\left(\frac{1}{\varepsilon} - \frac{r^2(t)e^{2\varphi(t)\mathbf{i}}}{2+\varepsilon}\right) = \left(\frac{1}{\varepsilon} - \frac{1}{2+\varepsilon}\right)\left\{(1-t) + te^{(2k+1)\varepsilon\pi\mathbf{i}}\right\}, \quad t \in [0,1], \\ r(0) = 1, \quad \varphi(0) = 0. \end{cases} \tag{6.3}$$

If $(2k+1)\varepsilon$ is an integer, a continuous solution to (6.3) corresponds to the real axis. Such a trajectory must go through the origin. Since we are concerned about classical solutions, this solution, if it exists, is excluded from our discussion.

Hence, we consider the case that $(2k+1)\varepsilon$ is not an integer. By conjugation, we need only consider the case when the line segment from $g(e^{0\mathbf{i}})$ to $g(e^{(2k+1)\pi\mathbf{i}})$ lies in the upper-half plane. Then there are two branches, γ_k^+ and γ_k^-, of solutions to (6.3); for small $t > 0$, γ_k^+ lies on the upper-half plane and γ_k^- lies on the lower half plane.

For γ_k^-, we study the image, under g, of the set $\{re^{\mathbf{i}\theta} \mid r > 0, -2\pi < \theta < 0\}$. By studying the images, under g, of the half lines $e^{0\mathbf{i}}[0,\infty)$ and $e^{-2\pi\mathbf{i}}[0,\infty)$ and the circle $\infty e^{[-2\pi,0]\mathbf{i}}$, one checks that the map from $z \in \{re^{\mathbf{i}\theta} \mid r > 0, \theta \in (-2\pi, 0)\}$ to $g(z)$ is one-to one. Denote the inverse of this map by g_1^{-1}. Then the branch γ_k^- of the solution to (6.3) is the image, under g_1^{-1}, of the line segment from $g(e^{0\mathbf{i}})$ to $g(e^{(2k+1)\pi\mathbf{i}})$. This image lies completely outside of the unit circle and does not land at the point -1. Thus, γ_k^- is not a trajectory.

Next we consider γ_k^+, the branch of the solution to (6.3) that lies in the upper-half plane for small positive t. It is easy to see that γ_k^+ lies inside of the unit circle for small positive t. Let K be as in the statement of Proposition 6.3. One notices the following:

(i) The map from z to $g(z) = z^\varepsilon(1/\varepsilon - z^2/(2+\varepsilon))$ is one-to-one on

$$D_K := \{re^{\mathbf{i}\theta} \mid 0 < r < 1, 0 < \theta < (4K-1)\pi\}.$$

(ii) The image $g(D_K)$ contains the sector

$$\{re^{\mathbf{i}\theta} \mid 0 < r < \tfrac{1}{\varepsilon} - \tfrac{1}{2+\varepsilon},\ 0 < \theta < (4K-1)\varepsilon\pi\}.$$

Indeed, both facts can be shown by checking the image, under g, of the boundary of the unit circle $\{re^{\mathbf{i}\theta} \mid 0 < r < 1, 2l\pi < \theta < (2l+2)\pi\}$ for $l = 0, \ldots, 2K-1$. We denote the inverse by g_*^{-1}. Since it is assumed that the line segment $\{tg(e^{0\mathbf{i}}) + (1-t)e^{(2k+1)\mathbf{i}}) \mid 0 < t < 1\}$ lies in the upper-half plane, it lies in $g(D_K)$. Hence, γ_k^+ is the image, under g_*^{-1}, of the line segment $\{[\frac{1}{\varepsilon} - \frac{1}{2+\varepsilon}][(1-t) + te^{(2k+1)\varepsilon\pi\mathbf{i}}] \mid t \in [0,1]\}$. It is then relatively easy to show that γ_k^+ ends at -1 if and only if $0 < (2k+1)\varepsilon < 1$ (always keeping in mind the assumption that the line segment from $g(e^{0\mathbf{i}})$ to $g(e^{(2k+1)\pi\mathbf{i}})$ lies in the upper-half plane). In addition, when $0 < (2k+1)\varepsilon < 1$, we have $r(t) \in (0,1)$ and $\varphi(t) \in (0, (2k+1)\pi)$ for all $t \in (0,1)$ and $\varphi(1) = (2k+1)\pi$. That is, γ_k^+ makes $k + 1/2$ loops around the origin and lies completely inside the unit circle. □

Finally, we remark that for $\varepsilon = 0$, this potential reduces to the one in Example 4 with $a = 1$, which does not have solutions with loops around the origin. Actually, loop

https://doi.org/10.1017/S095679250600667X Published online by Cambridge University Press

solutions for positive ε approach, as $\varepsilon \searrow 0$, $(2k+1)$ copies of the connection in the limit problem.

The analysis and conclusion for this example extends easily to the case $W = |(z^n - 1)z^{\varepsilon-1}|^2$ for any $\varepsilon \in (0,1)$ and integer $n \geqslant 2$.

For the purpose of applications, we provide examples of triple wells.

Example 7. $W(z) = \left|\dfrac{z^3+1}{z^3-1}\right|^2$.

To avoid the use of multiple-valued functions and to make our presentation as simple as possible, we shall utilize the following symmetries of the potential: (i) The potential is invariant under $\frac{2k\pi}{3}$ rotation (k integer) so that if z is a trajectory, so is $e^{2k\pi/3}z$. (ii) The potential is invariant under conjugation, $\overline{W(z)} = W(\bar{z})$ so that if γ is a trajectory, then its complex conjugate (reflection about the real line) is also a trajectory.

Now let γ be a trajectory to (1.1) that connects two wells, that is, two roots of $W = 0$. Since any of the three lines $e^{k\pi\mathbf{i}/3}\mathbb{R}$, $k = 1,2,3$ are trajectories, by uniqueness γ cannot intersect any of them in a tangential manner. Also, as it turns out, γ stays away from the origin. Hence, we can divide γ into finitely many pieces, γ_j, $j = 0,\ldots,m$, each piece lying in one of the six sectors $\{z \mid \mathrm{Arg}(z) \in [k\pi/3,(k+1)\pi/3]\}$, $k = 0,1,\ldots,5$. Now using rotation and conjugation, we can map each γ_i uniquely to a corresponding piece γ_i^* in the sector

$$D := \{z \mid \mathrm{Arg}(z) \in [0,\pi/3]\} \setminus \{1\}. \tag{6.4}$$

These new pieces are trajectories and have the following properties: (i) γ_0^* starts and γ_m^* ends at $e^{\pi\mathbf{i}/3}$; (ii) for $i = 1,\ldots,m-1$, the last point q_i of γ_i^* is the first point of γ_{i+1}^* and q_i lies either in $(0,1)\cup(1,\infty)$ or in $e^{\pi\mathbf{i}/3}((0,1)\cup(1,\infty))$. In addition, their tangent lines at q_i are symmetric about the normal line of the boundary of the sector D at q_i.

Now let g be one of the antiderivatives of f defined in the sector D. Then for each i, $L_i := g(\gamma_i^*)$ is a line segment in $g(D)$ with end points on $\partial g(D) = g(\partial D)$ (by the open mapping theorem of analytic functions). In addition, $g(\gamma_i^*)$ and $g(\gamma_{i+1}^*)$ share a common point $p_i := g(q_i)$ at the boundary of $g(D)$ and are symmetric about the normal line of $g(\partial D)$ at p_i, since g is a conformal mapping. Thus, finding a solution to (1.1) is equivalent to finding a finite sequence of line segments $\{L_i\}_{i=0}^m$ in $g(D)\cup\partial g(D)$, with the properties just mentioned above.

Now we pick a special antiderivative g of f in D. For convenience, we denote the poles and the zeroes of W by

$$p_0 = 1, \quad p_1 = e^{2\pi\mathbf{i}/3}, \quad p_2 = e^{-2\pi\mathbf{i}/3}, \quad z_0 = -1, \quad z_1 = e^{\pi\mathbf{i}/3}, \quad z_2 = e^{-\pi\mathbf{i}/3}.$$

We take

$$f(z) = \frac{z^3+1}{z^3-1} = 1 + \frac{2}{3}\sum \frac{p_j}{z-p_j},$$
$$g(z) := \int_0^z f(\zeta)\,d\zeta = z + \frac{2}{3}\sum p_j \log\left(1 - \frac{z}{p_j}\right) \qquad \forall z \in D.$$

where we use the branch of the logarithm $\log[re^{\mathbf{i}\theta}] = \log r + \mathbf{i}\theta$ for all $r > 0$ and $\theta \in [0,2\pi)$.

https://doi.org/10.1017/S095679250600667X Published online by Cambridge University Press

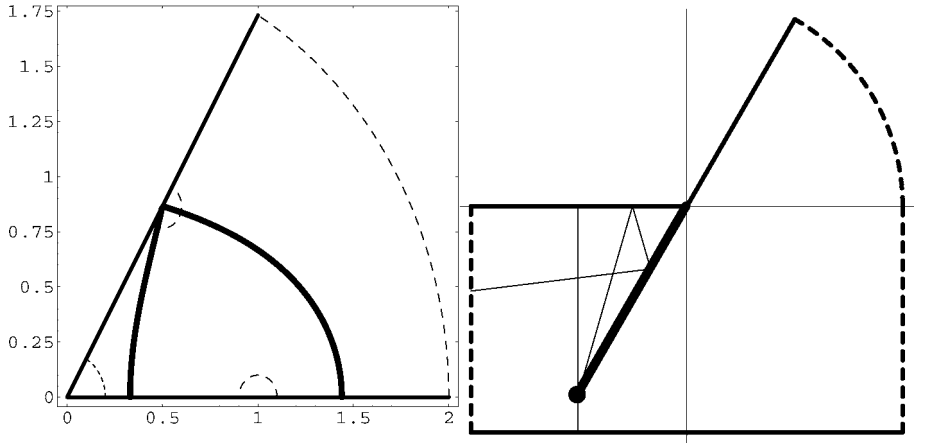

FIGURE 7. The map $z \to g(z)$ in Example **7**. The doted circular part on z plane corresponds to dotted parts on the $\zeta = g(z)$ plane. The two thick curves on the z plane are halves of two trajectories, one inside the circle, the other other outside the unit circle. Their image on the $\zeta = g(z)$ plane are the vertical line segments connecting the thick dashes. The preimage of the three thin line segments is not a homoclinic orbit.

We now investigate the image of the boundary of D (defined in (6.4)) under the mapping g. We divide the boundary of D into seven segments,

$$(1,\infty),\ 1+0e^{\mathbf{i}[0,\pi]},\ [0,1),\quad e^{\pi\mathbf{i}/3}[0,1),\ e^{\pi\mathbf{i}/3}(1+0e^{-[\pi,0]\mathbf{i}}),\ e^{\pi\mathbf{i}/3}(1,\infty),\ \infty e^{\mathbf{i}[0,\pi/3]}.$$

Their images are calculated as follows; see Figure 7.

(i) $g([1,\infty)) = -\frac{2}{3}\pi\mathbf{i} + \mathbb{R}$ (the line at the bottom);

(ii) $g(1+0e^{\mathbf{i}[0,\pi]}) = -\infty + \mathbf{i}[-\frac{2}{3}\pi, 0]$ (the dashed line on the left);

(iii) $g((0,1)) = (-\infty, 0)$ (the negative real axis);

(iv) $g(e^{\pi\mathbf{i}/3}(0,1]) = e^{-2\pi\mathbf{i}/3}(0,a_0]$ where $a_0 := \frac{2\sqrt{3}\pi}{9} + \frac{\ln 4}{3} - 1 \approx 0.67$ (we caution the reader that the actual bottom line $-2\pi/3 + \mathbb{R}$ lies much lower than plotted in the figure);

(v) $g(e^{\pi\mathbf{i}/3} + 0e^{[-2\pi/3,\pi/3]\mathbf{i}}) = a_0 e^{-2\pi\mathbf{i}/3} + 0e^{[-5\pi/3,\pi/3]\mathbf{i}}]$ (the small disk);

(vi) $g(e^{\pi\mathbf{i}/3}[1,\infty)) = e^{\pi\mathbf{i}/3}[-a_0,\infty)$;

(vii) $g(\infty e^{[0,\pi/3]\mathbf{i}}) = \infty e^{[0,\pi/3]\mathbf{i}}$ (the dashed line and arc on the right).

Thus, $g : D \to g(D)$ is one-to-one. The boundary of $g(D)$ consists of the full line $l_1 := -\frac{2}{3}\pi\mathbf{i} + \mathbb{R}$, the half line $l_2 = e^{-\pi\mathbf{i}}(0,\infty)$, the line segment $l_3 = e^{-2\pi\mathbf{i}/3}[0,a_0]$, and the half line $l_4 = l_3 \cup e^{\pi\mathbf{i}/3}(0,\infty)$. Here l_3 should be regarded as lying above l_4.

Now any solution to (1.1) corresponds to a finite sequence $\{L_j\}_{j=0}^m$ of line segments in $g(D)$ with end points on $g(\partial D) = \partial g(D) = \cup_{i=1}^4 l_i$ that have the following properties:

(1) L_0 begins and L_m ends at $a_0 e^{-2\pi\mathbf{i}/3}$;

(2) For $i = 1,\ldots,m-1$, L_i ends and L_{i+1} begins at the same point p_i on $\cup_{i=1}^4 l_i$. In addition, L_i and L_{i+1} are locally symmetric about the normal line of $\cup_{i=1}^4 l_i$ at p_i.

Upon checking all the possibilities, we can show that there are exactly two options:

https://doi.org/10.1017/S095679250600667X Published online by Cambridge University Press

(1) $m = 1$, both L_0 and L_1 are the same vertical line segments from $a_0 e^{-2\mathbf{i}\pi/3}$ to the real line.

(2) $m = 1$, both L_0 and L_1 are the same vertical line segments from $a_0 e^{-2\mathbf{i}\pi/3}$ to $-\frac{2}{3}\pi\mathbf{i} + \mathbb{R}$.

One can verify that (1) and (2) correspond to two different trajectories, denoted by γ_1 and γ_2 respectively. Both connect $e^{-\pi\mathbf{i}/3}$ and $e^{\pi\mathbf{i}/3}$, are symmetric about the real line, and lie in the sector $\{re^{\theta\mathbf{i}} \mid r > 0, |\theta| < \pi/3\}$; see Figure 7 for γ_1 and γ_2 restricted on D.

To see the relative position of γ_1 and γ_2 with respect to the unit circle, we find the image of the unit circle under g. For $\theta \in (0, \pi/3)$,

$$g(e^{\mathbf{i}\theta}) = g(e^{\pi\mathbf{i}/3}) + \int_{\pi/3}^{\theta} \frac{(e^{3\mathbf{i}\theta} + 1)de^{\mathbf{i}\theta}}{e^{3\mathbf{i}\theta} - 1} = a_0 e^{-2\pi\mathbf{i}/3} - \int_{\theta}^{\pi/3} \frac{2\sin(3\theta)(\cos\theta + \mathbf{i}\sin\theta)}{|2\sin(3\theta/2)|^2}\, d\theta.$$

Thus, the image of the circular parts $e^{\mathbf{i}\theta}$, $0 < \theta < \pi/3$, under g, is an increasing curve from $-\frac{2\pi}{3}\mathbf{i} - \infty$ to $a_0 e^{-2\pi\mathbf{i}/3}$. This implies that γ_1 lies inside the unit circle, and that γ_2 lies outside the unit circle. In summary, we have the following.

Proposition 6.4 *Assume that* $W(z) = \left|\frac{z^3+1}{z^3-1}\right|^2$. *Then,*

(i) (1.1) *does not have any non-trivial homoclinic orbits.*

(ii) *Between any pair of different roots of* $W = 0$, *there are exactly two connections of (1.1). These connections lie inside the sector determined by the pair of roots, and one of them,* γ_1, *lies inside the unit circle while the other,* γ_2, *lies outside of the unit circle. Their respective energies are*

$$E(\gamma_1) = 2a_0 \sin\frac{\pi}{3} = \frac{2\pi}{3} - \left(\sqrt{3} - \frac{\ln 4}{\sqrt{3}}\right),$$
$$E(\gamma_2) = \frac{4\pi}{3} - E(\gamma_1) = \frac{2\pi}{3} + \left(\sqrt{3} - \frac{\ln 4}{\sqrt{3}}\right) > E(\gamma_1).$$

To reduce the singularity of the potential just studied, we now consider the following.

Example 8. $W(z) = |(z^3+1)(z^3-1)^{-\alpha}|^2,\ 0 < \alpha < 1.$

Define D as in (6.4). As before, we need only to find a finite sequence of line segments in $g(D)$ that are obtained from a sequence of reflections about the boundary of $g(D)$, of light rays that begin and end at the same point $g(e^{\pi\mathbf{i}/3})$.

We adapt the convention

$$\mathrm{Arg}(z^3 - 1) \in [0, \pi] \qquad \forall z \in D,$$

and take

$$(re^{\mathbf{i}\theta})^{-\alpha} = r^{-\alpha} e^{-\alpha\theta\mathbf{i}},$$
$$f(z) = (z^3+1)(z^3-1)^{-\alpha},$$
$$g(z) = \int_0^z f(\zeta)\, d\zeta \qquad \forall z \in D.$$

We calculate the value of g on ∂D (cf. Figure 8).

https://doi.org/10.1017/S095679250600667X Published online by Cambridge University Press

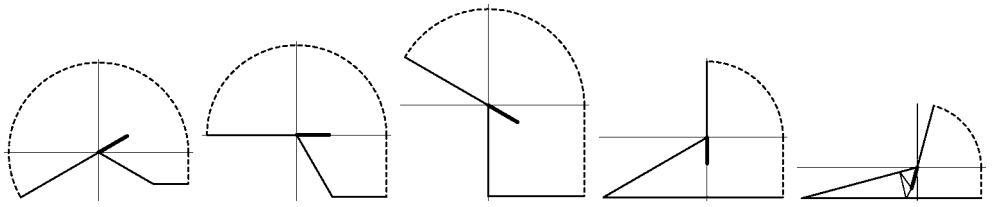

FIGURE 8. The image of the boundary $g(\partial D)$, with different values of α. From left to right: $\alpha = 1/6, 1/3, 1/2, 5/6, 11/12$. In the rightmost figure, the preimage of the light line segment corresponds to a homoclinic orbit that cover three copies of the region D.

(i) $g(e^{\pi \mathbf{i}/3}[1,\infty)) = e^{(4/3-\alpha)\pi \mathbf{i}}(-b_0,\infty) := l_1$, $b_0 := \int_0^1 (1-r^3)(1+r^3)^{-\alpha} dr$.

(ii) $g(e^{\pi \mathbf{i}/3}[0,1]) = e^{(1/3-\alpha)\pi \mathbf{i}}[0,b_0] =: l_2$; in particular, $g(e^{\pi \mathbf{i}/3}) = b_0 e^{(1/3-\alpha)\pi \mathbf{i}}$.

(iii) $g([0,1]) = e^{-\alpha\pi \mathbf{i}}[0,a_0] =: l_3$, $a_0 := \int_0^1 (r^3+1)(1-r^3)^{-\alpha} dr$.

(iv) $g([1,\infty)) = a_0 e^{-\alpha\pi \mathbf{i}} + [0,\infty) =: l_4$;

(v) $g(\infty e^{\mathbf{i}[0,\pi/3]}) = \infty e^{\mathbf{i}[0,(4/3-\alpha]\pi} =: l_5$ (the dashed arc).

Here one should regard l_2 as if it was below l_1 for $\alpha < 5/6$ and above for $\alpha > 5/6$.

Next we show that $g(e^{\pi \mathbf{i}/3}) = b_0 e^{(1/3-\alpha)\pi \mathbf{i}}$ lies above l_4 (this is not obvious in the case $\alpha > 1/3$) so that $g(D)$ is a domain bounded by $l_1, \ldots, l_5$ and that $z \in D \to g(z)$ is one-to-one. For this, we need only to show the positivity of the imaginary part of

$$\begin{aligned} Z &:= b_0 e^{(1/3-\alpha)\pi \mathbf{i}} - a_0 e^{-\alpha\pi \mathbf{i}} = g(e^{\pi \mathbf{i}/3}) - g(1) \\ &= \int_0^{\pi/3} (e^{3\mathbf{i}\theta}+1)(e^{3\mathbf{i}\theta}-1)^{-\alpha} de^{\mathbf{i}\theta}. \end{aligned}$$

Using $e^{3\theta \mathbf{i}} - 1 = 2\sin(3\theta/2) e^{(\pi+3\theta)\pi \mathbf{i}/2}$ we obtain

$$\begin{aligned} Z &= 2^{1-\alpha} \int_0^{\pi/3} \left\{ \sin \frac{\alpha\pi + 3\alpha\theta - 5\theta}{2} + \mathbf{i} \cos \frac{\alpha\pi + 3\alpha\theta - 5\theta}{2} \right\} \sin^{-\alpha} \frac{3\theta}{2} \cos \frac{3\theta}{2} \, d\theta \\ &= \frac{2^{2-\alpha}}{3} \int_0^{\pi/2} \left\{ \sin\left(\frac{\alpha\pi}{2} + \alpha\theta - \tfrac{5\theta}{3} \right) + \mathbf{i} \cos\left(\frac{\alpha\pi}{2} + \alpha\theta - \frac{5\theta}{3} \right) \right\} \sin^{-\alpha} \theta \cos\theta \, d\theta. \end{aligned}$$

Note that when θ increases from 0 to $\pi/2$, $\cos\theta \sin^{-\alpha}\theta$ decreases from $+\infty$ to 0, and $\frac{1}{2}\alpha\pi + \alpha\theta - \frac{5}{3}\theta$ decreases from $\alpha\pi/2 > 0$ to $\alpha\pi - 5\pi/6 > -\pi$. From this, we conclude that

$$\mathrm{Im}(Z) = \frac{2^{2-\alpha}}{3} \int_0^{\pi/2} \cos\left(\frac{\alpha\pi}{2} + \alpha\theta - \frac{5\theta}{3} \right) \sin^{-\alpha}\theta \cos\theta \, d\theta > 0.$$

Clearly, the orthogonal projection from $g(e^{\pi \mathbf{i}/3}) = b_0 e^{(1/3-\alpha)\pi \mathbf{i}}$ onto l_3 gives us a trajectory γ_1, whose energy is

$$E(\gamma_1) = 2b_0 \sin(\pi/3) = \sqrt{3} \int_0^1 (1-r^3)(1+r^3)^{-\alpha} \, dr.$$

https://doi.org/10.1017/S095679250600667X Published online by Cambridge University Press

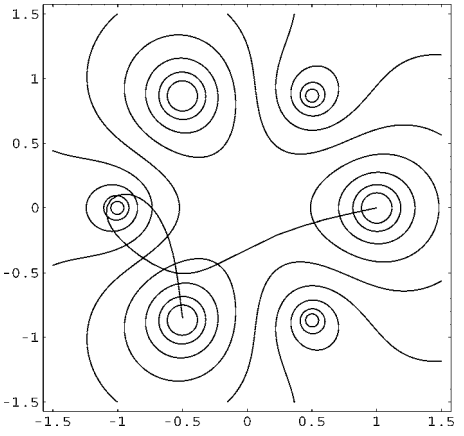

FIGURE 9. A trajectory connecting two wells and making one loop around a pole, $\alpha = 7/10$.

If the orthogonal projection from $g(e^{\pi \mathbf{i}/3})$ to l_4 does not intersect l_3, namely

$$\mathrm{Re}(Z) = \frac{2^{2-\alpha}}{3} \int_0^{\pi/2} \sin\left(\frac{\alpha\pi}{2} + \alpha\theta - \frac{5\theta}{3}\right) \sin^{-\alpha}\theta \cos\theta \, d\theta > 0 \Leftrightarrow \alpha > \alpha_* = 0.35699\ldots$$

then we have another trajectory, γ_2, whose energy is

$$E(\gamma_2) = 2\,\mathrm{Im}(Z).$$

The position of $g(e^{\pi \mathbf{i}/3})$ is of importance here. We can deduce the following facts:

(i) For $0 < \alpha < \alpha_* = 0.35699\ldots$, the vertical projection of $g(e^{\pi \mathbf{i}/3})$ onto l_4 intersects l_3, so there exists only one trajectory, γ_1, being the preimage, under g, of the projection line segment from $g(e^{\pi \mathbf{i}/3})$ onto l_3.

(ii) For $\alpha_* < \alpha < 1$, the vertical projection of $g(e^{\pi \mathbf{i}/3})$ does not intersects l_3, so there are two trajectories, γ_1 obtained from the preimage, under g, of the projection of $g(e^{\pi \mathbf{i}/3})$ onto l_3 and γ_2 from that onto l_4. A numerical evaluation clearly shows that $E(\gamma_2) > 2E(\gamma_1)$.

(iii) For $\alpha = \alpha^*$, γ_2 becomes singular since it passes through the pole 1 of the potential.

(iv) For α close to 1, looped trajectories can be constructed; see Figure 8e and Figure 9.

The image of the unit circle in D is given by

$$g(e^{\mathbf{i}\varphi}) = g(e^{\pi \mathbf{i}/3}) - 2^{1-\alpha} \int_{\varphi}^{\pi/3} \left\{ \sin\frac{\alpha\pi + 3\alpha\theta - 5\theta}{2} + \mathbf{i}\cos\frac{\alpha\pi + 3\alpha\theta - 5\theta}{2} \right\} \sin^{-\alpha}\frac{3\theta}{2} \cos\frac{3\theta}{2} d\theta$$

for $\varphi \in (0, \pi/3)$. (a) It is a curve beginning at $b_0 e^{(1/3-\alpha)\pi \mathbf{i}}$ with tangent parallel to l_1, and finishing off at $a_0 e^{-\alpha\pi}$ with tangent lying in the middle of l_3 and l_4. (b) For $\alpha \in [5/6, 1)$, it always goes to the left; when $\alpha \in (0, 5/6)$, it first swings to the right, and then goes to the left, changing its direction at the zero of $\alpha\pi + 3\alpha\theta^* - 5\theta^* = 0$, i.e., at $\theta^* = \alpha\pi/(5 - 3\alpha)$. (c) When $1 > \alpha \geqslant 1/3$, it always goes downwards; when $0 < \alpha < 1/3$, it first goes up and then goes down, changing its course at $\theta = \frac{1+\alpha}{5-3\alpha}\pi$. Thus, when $\alpha \in [\frac{5}{6}, 1)$, γ_2 does not intersect the unit circle, whereas when $\alpha < 5/6$, γ_2 intersects the unit circle twice, at $e^{\mathbf{i}\hat{\theta}}$

https://doi.org/10.1017/S095679250600667X Published online by Cambridge University Press

and $e^{-\hat{\theta}\mathbf{i}}$, respectively, for some $\hat{\theta} \in (0, \theta^*)$. The middle part lies outside of the unit circle, and the head and tail parts (those joining $e^{\pm 2\pi\mathbf{i}/3}$) lie inside the circle. Finally, γ_1 lies inside of γ_2 and the unit circle.

Proposition 6.5 *Let* $W(z) = |(z^3+1)(z^3-1)^{-\alpha}|^2$, $0 < \alpha < 1$. *Let* $\alpha^* \approx 0.35699$ *be the root to* $Re(Z) = 0$.

(i) *For* $\alpha \in (0, \alpha^*]$, *there is exactly one trajectory connecting* $e^{\pi\mathbf{i}/3}$ *and* $e^{-\pi\mathbf{i}/3}$.

(ii) *For* $\alpha \in (\alpha^*, 1)$, *(1.1) admits two trajectories connecting* $e^{\pi\mathbf{i}/3}$ *and* $e^{-\pi\mathbf{i}/3}$; *one of them,* γ_1, *lies inside the unit circle, whereas the other,* γ_2, *lies outside of* γ_1 *and the pole. When* $\alpha \in (5/6, 1)$, γ_2 *lies completely outside of the unit circle, whereas when* $\alpha \in (\alpha^*, 5/6)$, γ_2 *intersects the unit circle exactly twice. Their energies are respectively*

$$E(\gamma_1) = \sqrt{3}b_0, \quad E(\gamma_2) = 2\mathrm{Im}(Z) = 2\{(b_0 \sin((1/3-\alpha)\pi) + a_0 \sin \alpha\pi\} > 2E(\gamma_1).$$

(iii) For α *close to* 1, *there are looped trajectories with the number of loops increasing to* ∞ *as* α *increases to* 1.

We remark the following:

(1) The existence of a unique α^* is established by showing numerically that the derivative of the function $\alpha \to \mathrm{Re}(Z)$ is positive.

(2) Similarly, numerical evaluation gives $\inf_{\alpha \in (\alpha^*, 1)} \frac{E\gamma_2)}{E(\gamma_1)} > 2.1$, and so we conclude that $E(\gamma_2) > 2E(\gamma_1)$. Finding an analytical proof appears too hard for the moment and also not necessary.

(3) The third assertion (iii) is proved by finding the number of ways that a light ray, emitted from $g(e^{\pi\mathbf{i}/3})$, travelling in $g(D)$, bouncing back and forth at the boundary of $g(D)$, can end at $g(e^{\pi\mathbf{i}/3})$; see Figure 8e. We omit the details.

Finally, we consider the potential that was first used in our numerical simulation.

Example 9. $W(z) = |z^3-1|^2|z^3+\alpha^3|^{-1}$, $\alpha \in (0, \infty)$.
As before, we let D as in (6.4) and set

$$f(z) = \frac{z^3-1}{\sqrt{\alpha^3+z^3}}, \quad g(z) = \int_0^z f(\zeta)\, d\zeta \quad z \in D.$$

The image $g(\partial D)$ can be calculated as follows (see Figure 10).

(i) $g([0,\infty)) = [-a_0, \infty)$, $\quad a_0 = \int_0^1 \frac{1-r^3}{\sqrt{\alpha^3+r^3}}\, dr$.

(ii) $g([0,\alpha]e^{\pi\mathbf{i}/3}) = e^{4\pi\mathbf{i}/3}[0, b_0] =: l_3$, $\quad b_0 := \int_0^\alpha \frac{1+r^3}{\sqrt{\alpha^3-r^3}}\, dr$.

(iii) $g([\alpha,\infty)e^{\pi\mathbf{i}/3}) = g(\alpha e^{\pi\mathbf{i}/3}) + e^{5\pi\mathbf{i}/6}[0,\infty) =: l_4$.

(iv) $g(\infty e^{[0,\pi/3]\mathbf{i}}) = \infty e^{[0,5\pi/6]\mathbf{i}}$.

https://doi.org/10.1017/S095679250600667X Published online by Cambridge University Press

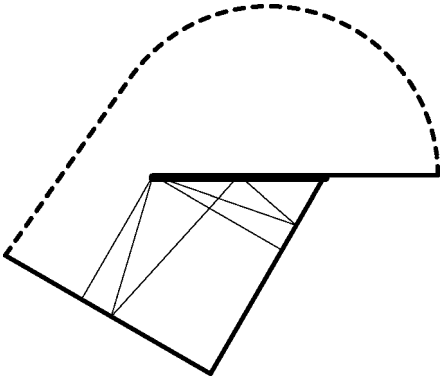

FIGURE 10. The image $g(\partial D)$ in Example **9**. The thick dotted and solid curves are the image of $g(\partial D)$. The preimage of the thin line segments provide homoclinic connections.

We claim that $g(1) = -a_0$ lies above the l_4 line segment. For establishing this it is sufficient to show that $\frac{1}{2}a_0 < b_0$. We calculate

$$\begin{aligned} 2b_0 - a_0 &= 2\int_0^1 \frac{1+\alpha^3\rho^3}{\sqrt{\alpha}\sqrt{1-\rho^3}}\,d\rho - \int_0^{1/\alpha} \frac{1-\alpha^3\rho^3}{\sqrt{\alpha}\sqrt{1+\rho^3}}\,d\rho \\ &> \frac{1}{\sqrt{\alpha}}\Big(\int_0^1 \frac{2}{\sqrt{1-\rho^3}}\,d\rho - \int_0^{\infty} \frac{1}{\sqrt{1+\rho^3}}\,d\rho\Big) = 0. \end{aligned}$$

Hence, g maps D in one-to-one manner onto its image $g(D)$. Let γ_1 be the pre-image of the projection line segment from $g(1)$ to l_3 and let γ_2 be that from $g(1)$ to l_4. Then both γ_1 and γ_2 are half trajectories connecting 1 and $e^{2\pi\mathbf{i}/3}$; γ_2 lies outside the pole $\alpha e^{\pi\mathbf{i}/3}$ whereas γ_1 lies inside the pole $\alpha e^{\pi\mathbf{i}/3}$. Their corresponding energies are given by

$$E(\gamma_1) = \sqrt{3}a_0, \qquad E(\gamma_2) = 2b_0 - a_0.$$

In terms of $\alpha \in (0,\infty)$, numerical evaluation shows that there exists a unique $\alpha^* = 0.55707\ldots$ such that

$$E(\gamma_1) < E(\gamma_2) \ \text{ when } \ \alpha > \alpha^*, \qquad E(\gamma_1) > E(\gamma_2) \ \text{when } \ \alpha \in (0,\alpha^*). \tag{6.5}$$

From Figure 10 and using Euclidean geometry, one can prove that there are also looped trajectories. We omit the details. We summarize our conclusions as follows:

Proposition 6.6 *Let* $W = |z^3-1|^2\,|z^3+\alpha^3|^{-1}$, $\alpha > 0$. *There are exactly two trajectories,* γ_1 *and* γ_2, *that connect* 1 *and* $e^{2\pi\mathbf{i}/3}$ *and lie in the sector* $0 < \mathrm{Arg}(z) < 2\pi/3$;. *In addition,*

(i) γ_1 *lies inside of the domain bounded by* γ_2 *and line segments* $[0,1] \cup e^{2\pi\mathbf{i}/3}[0,1]$ *and the pole* $\alpha e^{\pi\mathbf{i}/3}$ *lies inside of the domain bounded by* $\gamma_1 \cup \gamma_2$;

(ii) *if* $\gamma \neq \gamma_1, \gamma_2$, *is a trajectory connecting* 1 *and* $e^{2\pi\mathbf{i}/3}$, *then* $E(\gamma) > \max\{E(\gamma_1), E(\gamma_2)\}$.

(iii) *there exists a number* $\alpha^* \approx 0.55707$ *such that (6.5) holds.*

https://doi.org/10.1017/S095679250600667X Published online by Cambridge University Press

7 Numerical simulations for the interfacial dynamics

The goal here is to design an algorithm and use it to observe numerically the evolution of interfaces of the vector Allen-Cahn dynamics modelling grain boundaries. We would like to find and to understand how different classes of interfaces are formed and how do they evolve and interact with each other.

7.1 The model

For definiteness, we consider the Allen-Cahn system

$$\begin{cases} u_t(x,y,t) = \epsilon^2 \Delta u - W_u(u,v), \\ v_t(x,y,t) = \epsilon^2 \Delta v - W_v(u,v), \end{cases} \qquad (x,y) \in \mathbb{R}^2,\ t > 0 \tag{7.1}$$

with periodic boundary conditions, for $\mathbf{u} = (u,v)$,

$$\mathbf{u}(x+1,y,t) = \mathbf{u}(x,y+1,t) = \mathbf{u}(x,y,t), \quad (x,y) \in \mathbb{R}^2, t \geqslant 0. \tag{7.2}$$

We use the potential

$$W(u,v) = \frac{|z^3-1|^2}{|z^3+\alpha^3|}, \qquad z = u + \mathbf{i}v, \quad \alpha > 0,$$

with which (1.1) admits exactly two distinct non-looped connections between each pair of wells of the set $\{1, e^{2\pi\mathbf{i}/3}, e^{-2\pi\mathbf{i}/3}\}$; see Example **9** in the previous section. Here the positive parameter α regulates the balance for the two energies (defined in (1.2)) of the two connections. The energy $E(\mathbf{U})$ of a connection $\mathbf{U}$ is typically called the interfacial energy density since in the direction perpendicular to an interface, $\mathbf{u}$ in (7.1) is approximately equal to a scaled version of $\mathbf{U}$, so that, since ϵ is small, there is the approximation of the total energy

$$\iint_{\Omega} \left\{ \frac{\epsilon}{2} |\nabla \mathbf{u}|^2 + \frac{1}{\epsilon} W(\mathbf{u}) \right\} dx\, dy \approx \sqrt{2} \int_I E(\mathbf{U})\, d\ell$$

where I is the interface in Ω, $d\ell$ is the arc length parameter, and $E(\mathbf{U})$ is the energy of the connection used by $\mathbf{u}$ in the cross section of the interface.

7.2 Discretization

We discretize the equations by an explicit forward in time and centered in space finite difference scheme, with a fixed uniform spatial mesh size h and dynamic time steps $k(0), k(1), \ldots$. Denote by $\mathbf{u}_{ij}^n = (u_{ij}^n, v_{ij}^n)$ the numerical approximation of $\mathbf{u}$ at $x_i = ih, y_j = jh$ and $t_n = \sum_{m=0}^{n-1} k(m)$ ($t_0 = 0$). The discrete equations are

$$\mathbf{u}_{ij}^* = \mathbf{u}_{ij}^n + \frac{k\epsilon^2}{2} \Delta_{ij} \mathbf{u}^n - \frac{k}{2} W_{\mathbf{u}}(\mathbf{u}_{ij}^n),$$
$$\mathbf{u}_{ij}^{n+1} = u_{ij}^n + k\epsilon^2 \Delta_{ij} u^* - k W_{\mathbf{u}}(\mathbf{u}^*{}_{ij}),$$

https://doi.org/10.1017/S095679250600667X Published online by Cambridge University Press

where the partial derivatives of W are calculated using simple centered differences and the discrete operator Δ_{ij} is a centered, second order approximation of the Laplacian Δ, given by

$$\Delta_{ij}\phi = \frac{\phi_{i+1,j+1} + \phi_{i-1,j+1} + \phi_{i+1,j-1} + \phi_{i-1,j-1} + 4\left(\phi_{i+1,j} + \phi_{i-1,j} + \phi_{i,j+1} + \phi_{i,j-1}\right) - 20\phi_{i,j}}{6h^2}.$$

To ensure stability, the time-step k and spatial size h must satisfy the CF condition $h^2 > 4\epsilon^2 k$. For optimal accuracy, we require the change of the numerical solution $\mathbf{u}$ be less than a small percentage of $|\mathbf{u}|$ in each time update. Thus, we choose our dynamic time step by

$$k = k(n) = \min_{ij}\left(\frac{h^2}{4\epsilon^2}, \frac{|\mathbf{u}|}{100|\mathbf{u}_t|}\right).$$

Here we care more on the accuracy than on the efficiency and speed of the scheme.

7.3 Validation

In order to check that the scheme works correctly, we test the scheme by using one-dimensional solutions to

$$\epsilon^2 \mathbf{U}_{xx} = W_{\mathbf{u}}(\mathbf{U}) \text{ on } \mathbb{R}, \quad \mathbf{U}(-\infty) = (1,0), \quad \mathbf{U}(\infty) = (-\tfrac{1}{2}, \tfrac{\sqrt{3}}{2}). \tag{7.3}$$

We can obtain numerically desired solutions of this boundary value problem by shooting. First we linearize the equation in a neighborhood of the critical point $(1,0)$ to find four eigenmodes $\mathbf{v}_i e^{\lambda_i x}$, $i = 1,2,3,4$, where λ_i and $\mathbf{v}_i$ are the eigenvalue and the unit eigenvector of the corresponding characteristic system $\lambda^2 \mathbf{v} = \mathbf{v}\, W_{\mathbf{uu}}(1,0)$. We take the convention $\lambda_1 \geqslant \lambda_2 > 0$, $\lambda_3 = -\lambda_1$, $\mathbf{v}_3 = \mathbf{v}_1$, $\lambda_4 = -\lambda_2$ and $\mathbf{v}_4 = \mathbf{v}_2 \perp \mathbf{v}_1$. One can derive that

$$\mathbf{U}(x) = (1,0) + \delta\left\{\mathbf{v}_1 e^{\lambda_1 x}\cos\theta + \mathbf{v}_2 e^{\lambda_2 x}\sin\theta\right\} + O(\delta^2 e^{2\lambda_2 x}) \quad \forall\, x \leqslant 0.$$

Here the value $\theta \in [0, 2\pi)$ is not arbitrary. It is obtained by shooting. Note that the smallness of δ is equivalent to the translation of x. We use $(1,0) + 10^{-10}\{\mathbf{v}_1\cos\theta + \mathbf{v}_2\sin\theta\}$ as an initial data for the numerical solution $\mathbf{U}$ at $x = 0$ and integrate the ODE system (7.3) with a fourth order Runge-Kutta scheme. We adjust the parameter θ until the numerical solution $\mathbf{U}(x)$ arrives a tiny neighborhood of the critical point $(-1/2, \sqrt{3}/2)$ for certain large x. We obtain exactly two non-looped trajectories, plotted by the two solid curves in Figure 11.

In Figure 11, we also plot by dots two steady states $\mathbf{u}^*(x) = \lim_{t\to\infty}\mathbf{u}(x,y,t)$ of two numerical solutions of the PDE problem (7.1)–(7.2) with y independent initial values and with the aforementioned numerical scheme. The differences between $\mathbf{U}$ and $\mathbf{u}^*$ near the critical points are due to the fact that our initial value problems are solved in a bounded domain with periodic boundary conditions.

7.4 A numerical simulation

We start with a random initial data $\mathbf{u}(x,y,0)$ obtained from a pseudorandom number generator, and we wait until the interfaces develop. Taking $\alpha = 0.55$, in Figure 1 we

https://doi.org/10.1017/S095679250600667X Published online by Cambridge University Press

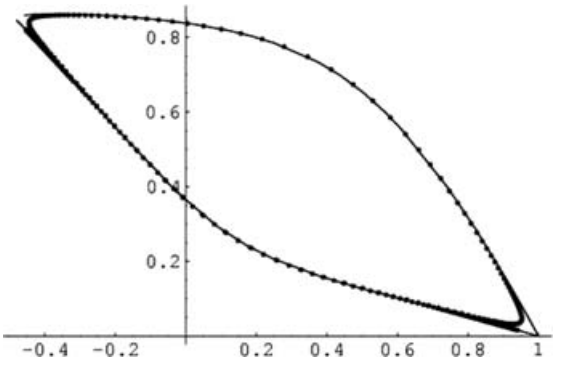

FIGURE 11. Comparison of the numerical steady states with planer interfaces of the PDE problem in a bounded domain with trajectories of the ODE problem.

provide three pairs of snapshots, taken at three different time moments, recording the interfaces (left column) and phase domains (right column). The observed phenomena of generation and evolution of interfaces are generic (e.g obey certain laws).

In each image on the left, the interfaces are painted in a way that distinguishes between the two different types. The grayscale depends on the value of $|\mathbf{u}|$; that is, a light gray interface corresponds to the connection $\mathbf{U}$ that is closer to the origin in Figure 11 whereas a black interface denotes the connection in Figure 11 that is farther from the origin. It is evident that the two classes of interfaces coexist at a given time. When $\alpha = 0.55$, the transition energy of the light grey interface is higher than that of the black one, so that during the evolution process, the proportion of the light gray interface gradually decreases. We can adjust α to make the two transition energies almost equal, in which case, the evolution of the proportion (not shown here) is observed to be very slow. We remark that the color at the junctions has no significance.

In each picture on the right column, we use three different grayscales to denote the three different phase regions: white for the region $\{(x, y) \mid \mathbf{u}(x, y, t) \sim 1\}$, grey for $\{\mathbf{u} \sim e^{2\pi \mathbf{i}/3}\}$ and black for $\{\mathbf{u} \sim e^{-2\pi \mathbf{i}/3}\}$.

8 Conclusions and open problems

We studied the solutions of $2\mathbf{u}_{xx} = W_u(\mathbf{u})$ where W is a potential with multiple global minima. This equation describes the equilibrium of interfaces of the solutions of the vector Allen-Cahn equations. In particular we developed a method that allows the construction of closed-form solutions for potentials of the form $W = |f(z)|^2$, which includes the usual symmetric three well potential. We show that for potentials of type I ($f(z)$ holomorphic) there exists at most one connection between any pair of wells, while for type II potentials ($f(z)$ meromorphic with poles), multiple connections between a pair of wells may exist. We also give examples of potentials for which a pair of wells does not have a connection. The most striking implication is that the Plateau conditions are not necessarily satisfied for equilaterally symmetric potentials. We verified numerically that these two kinds of interfaces can be developed spontaneously on the evolution of the Allen–Cahn equation starting with initial random data.

https://doi.org/10.1017/S095679250600667X Published online by Cambridge University Press

For a follow-up to this paper addressing the existence issue for potentials with several global minima, and also clarifying further the case of non-existence and its robustness under small perturbations, we refer to the recent work of Alikakos & Fusco [4]. There are a number of open problems that we did not discuss in this paper

- Equilibrium and stability of the triple junctions: the detailed analysis would consider the full two dimensional solutions to the elliptic system $\Delta u = W_u(\mathbf{u})$ (now we cannot reduce the problem to ODES). Is it possible to prove existence and stability of junctions with two different kinds of interfaces which have different connections far away from the triple point? For the elliptic system capturing the solution in the core of the junction we refer elsewhere [3, 13, 33]
- Dynamical issues: Our simulations for networks made up of interfaces of two kinds show a gradual conversion into one into one kind of interface, via a travelling wave motion on the interface itself. A rigorous result would be of interest, even for a simple arrangement of interfaces.
- Equilibrium of networks of multiple triple junctions: what are the possible steady states, for example, inside a convex domain with Neumann boundary conditions? Are hexagonal networks stable? Is the stability of the network affected by the existence of multiple connections? For the associated sharp interface problem we refer elsewhere [28, 35].
- Extension to the three dimensional case: we think that it is possible that many of our results hold in the three dimensional case, where now four interfaces can meet at a point. Are the Plateau conditions violated with a symmetric potential with singularities?
- Cahn–Hilliard dynamics: under certain conditions, it has the same steady states than the Allen–Cahn system [8]. However it would be interesting to study the dynamics to determine if two kinds of interfaces develop spontaneously as did in our numerical simulation of the time-dependent Allen–Cahn system.

Acknowledgments

Santiago Betelu and Nicholas Alikakos were partially supported by a grant from the University of North Texas. Xinfu Chen was partially supported by the National Science Foundation grant DMS-0203991.

References

[1] Alberti, G. & Bellettini, G. (1998) A nonlocal anisotropic model for phase transitions: Part I: the optimal profile problem. *Math. Ann.* **310**, 527–560.
[2] Alberti, G. & Bellettini, G. (1998) A non-local anisotropic model for phase transitions: asymptotic behaviour of rescaled energies. *Europ. J. Appl. Math.* **9**, 261–284.
[3] Alama, S., Bronsard, L. & Gui, C. (1997) Stationary layered solutions in $\mathbb{R}^2$ for an Allen-Cahn system with multiple well potential. *Calc. Var. P.D.E.* **5**, 359–390.
[4] Alikakos, N. & Fusco, G. (2006) The Connection Problem For Potentials With Several Global Minima. Preprint.
[5] Alikakos N., Betelú, S. and Chen, X. In preparation.
[6] Arnold, V. I. (1989) *Mathematical Methods of Classical Mechanics* 2nd edition, Graduate texts in mathematics, Springer Verlag.

[7] Arnold, V. I. (1991) *Ordinary Differential Equations*, Springer, pp. 164–188.
[8] Baldo, S. (1990) Minimal interface criterion for phase transitions in Mixtures of Cahn-Hilliard fluids. *Ann. Inst. Henri Poincare,* **7**(2), 67–90.
[9] Bates, P. W., Fife, P. C., Ren, X. & Wang, X. (1997) Traveling waves in a convolution model for phase transitions. *ARMA*, **138**, 105–136.
[10] Bates, P. W. & Chmaj, A. (1999) An integrodifferential model for phase transitions: stationary solutions in higher space dimensions. *J. Statist. Phys.* **95**, 1119–1139.
[11] Bates, P. W., Chen, X. & Chmaj, A. (2003) Traveling waves on a lattice. *SIAM J. Math. Anal.* **35**, 520–546.
[12] Bellettini, G., Buttà, P. & Presutti, E. (2001) Sharp interface limits for non-local anisotropic interactions. *ARMA*, **159**, 109–135.
[13] Bronsard, L., Gui, C. & Schatzman, M. (1996) A Three-Layered Minimizer in R2 for a variational Problem with a symmetric Three-Well potential. *Comm. Pure Appl. Math.* **49**, 677–715.
[14] Bronsard, L. & Reitich, F. (1993) On Three-Phase Boundary Motion and the singular limit of a Vector-Valued Ginzburg-Landau Equation. *ARMA*, **1240**, 355–379.
[15] Brandon, D. & Rogers, R. C. (1992) The coercivity paradox and nonlocal ferromagnetism. *Contin. Mech. Thermodyn.* **4**, 1–21.
[16] Bronsard, L. & Wetton, B. T. R. (1995) A Numerical Method for Tracking Curve Networks Moving with Curvature Motion. *J. Computational Phys.* **120**, 66–87.
[17] Cahn, J. W. & Hilliard, J. E. (1983) Free energy of a nonuniform system I. Interfacial free energy. *J. Chem. Phys.* **28**, 258–267.
[18] Chen, X. (1997) Existence, uniqueness, and asymptotic stability of traveling waves in nonlocal evolution equations. *Adv. Diff. Eq.* **2**, 125–160.
[19] Chmaj, A. & Ren, A. (1999) Homoclinic solutions of an integral equation: existence and stability. *J. Diff. Eq.* **155**, 17–43.
[20] Comets, F., Eisele, T. & Schatzman, M. (1986) Bifurcations for some nonlinear convolution equations. *Trans. Amer. Math. Soc.* **296**, 661–702.
[21] de Masi, A., Gobron, T. & Presutti, E. (1995) Traveling fronts in non-local evolution equations. *ARMA*, **132**, 143–205.
[22] Ermentrout, G. B. (1998) Neural networks as spatio-temporal pattern-forming systems. *Reports on Progress in Physics*, **61**, 353–430.
[23] Ermentrout, G. B. & McLeod, J. B. (1993) Existence and uniqueness of travelling waves for a neural network. *Proc. Roy. Soc. Edinburgh Sect. A*, **123**, 461–478.
[24] Fife, P. C. & McLeod, J. B. (1977) The approach of solutions of nonlinear diffusion equations to travelling front solutions. *ARMA*, **65**, 335–361.
[25] Giaquinta, M. &. Hildebrandt, S. (1996) *Calculus of variations Vol 2*, Springer.
[26] Griewank, A. & Rabier, P. J. (1990) On the smoothness of convex envelopes. *Trans. Am. Math. Soc.* **322**, 691–709.
[27] Hale, J. K. & Kogak, K. H. (1994) *Dynamics and Bifurcations*. Springer.
[28] Ikota, R. & Yanagida, E. (2005) Stability of Stationary Injterfaces of binary-Tree type. *Calc. Var.* **22**, 375–389.
[29] Kirchheim, B. & Kristensen, J. (2001) Differentiability of convex envelopes. *C. R. Acad. Sci. Paris Sér. I Math.* **333**, 725–728.
[30] Landau, L. D. & Lifshitz, E. M. (2002) *Mechanics*, third Edition, Butterworth-Heinemann.
[31] Mantegazza, M., Novaga, V. & Tortorelli, M. (2004) Motion by Curvature of Planar Networks. *Ann. Sc. Norm. Super. Pisa Cl. Sci.* **3**.
[32] Rowlinson, J. S. (1979) Translation of J.D. van der Waals' "The thermodynamic theory of capillarity under the hypothesis of a continuous variation of density". *J. Stat. Phys.* **20**, 197–244.
[33] Schatzman, M. (2002) Asymmetric Heteroclinic Double Layer. *ESAIM Control, Optimization and Calculus of Variations*, **8**, 965–1005.
[34] Sternberg, P. (1991) Vector-Valued local minimizers of nonconvex variational problems. *Rocky Mountain J. Math.* **21**(2).

[35] Sternberg, P. & Ziemer, W. (1994) Local minimisers of a three-phase transition problem with triple junctions. *Proc. R. Soc. Ed.* **124A**(6), 1059–1073.
[36] Widom, B. (1972) Surface tension of fluids. In: C. Domb and M. S. Green (eds.), *Phase Transitions and Critical Phenomena*, Vol. 2, Academic Press, pp. 79–100.
[37] Widom, B. (1999) What do we know that van der Waals did not know? STATPHYS 20 (Paris 1998). *Phys. A*, **263**, 500–515.
[38] Wang, X. (2002) Metastability and stability of patterns in a convolution model for phase transitions. *J. Diff. Eq.* **183**, 434–461.